

Chikungunya intra-vector dynamics in *Aedes albopictus* from Lyon (France) upon exposure to a human viremia-like dose range reveals vector barrier's permissiveness and supports local epidemic potential

Barbara Viginier¹, Lucie Cappuccio¹, Céline Garnier¹, Edwige Martin², Carine Maisse¹, Claire Valiente Moro², Guillaume Minard², Albin Fontaine^{3,4,5}, Sébastien Lequime⁶, Maxime Ratinier¹, Frédérick Arnaud¹ & Vincent Raquin*¹

1 IVPC UMR754, INRAE, Univ Lyon, Université Claude Bernard Lyon 1, EPHE, PSL Research University, F-69007 Lyon, France.

2 Univ Lyon, Université Claude Bernard Lyon 1, CNRS, INRAE, VetAgro Sup, UMR Ecologie Microbienne, F-69622 Villeurbanne, France.

3 Unité Parasitologie et Entomologie, Département Microbiologie et maladies infectieuses, Institut de Recherche Biomédicale des Armées (IRBA), Marseille, France.

4 Aix Marseille Univ, IRD, SSA, AP-HM, UMR Vecteurs-Infections Tropicales et Méditerranéennes (VITROME), Marseille, France.

5 IHU Méditerranée Infection, Marseille, France.

6 Cluster of Microbial Ecology, Groningen Institute for Evolutionary Life Sciences, University of Groningen, Groningen, The Netherlands.

*Corresponding author

Correspondence: vincent.raquin@ephe.psl.eu

ABSTRACT

Arbovirus emergence and epidemic potential, as approximated by the vectorial capacity formula, depends on host and vector parameters, including the vector's intrinsic ability to replicate then transmit the pathogen known as vector competence. Vector competence is a complex, time-dependent, quantitative phenotype influenced by biotic and abiotic factors. A combination of experimental and modelling approaches is required to assess arbovirus intra-vector dynamics and estimate epidemic potential. In this study, we measured infection, dissemination, and transmission dynamics of chikungunya virus (CHIKV) in a field-derived *Aedes albopictus* population (Lyon, France) after oral exposure to a range of virus doses spanning human viraemia. Statistical modelling indicates rapid and efficient CHIKV progression in the vector mainly due to an absence of a dissemination barrier, with 100% of the infected mosquitoes ultimately exhibiting a disseminated infection, regardless of the virus dose. Transmission rate data revealed a time-dependent, but overall weak, transmission barrier, with individuals transmitting as soon as 2 days post-exposure (dpe) and >50% infectious mosquitoes at 6 dpe for the highest dose. Based on these experimental intra-vector dynamics data, epidemiological simulations conducted with an agent-based model showed that even at low mosquito biting rates, CHIKV could trigger outbreaks locally. Together, this reveals the epidemic potential of CHIKV upon transmission by *Aedes albopictus* in mainland France.

NOTE: This preprint reports new research that has not been certified by peer review and should not be used to guide clinical practice.

41
42
43
44
45

Keywords: Arbovirus ; vector ; mosquito ; *Aedes albopictus* ; chikungunya virus ; epidemiology ; vector competence ; modelisation

Introduction

Arthropod-borne viruses (arboviruses) are pathogens transmitted to vertebrate hosts by hematophagous arthropods, mainly mosquitoes. Arbovirus spread is a multi-factorial, dynamic process that can be estimated using the vectorial capacity (VCap) model, which aims to determine the average number of infectious vector bites that arise per day from one infected host in a susceptible human population (Smith et al., 2012). The vector-centric component of VCap integrates mosquito ecological (density per host, survival) and behavioural (daily biting rate per human) factors along with the vector's proxies of virus transmission efficiency such as vector competence (VComp) and its time-related expression, the extrinsic incubation period (EIP). VComp represents the ability of mosquitoes to : i) allow midgut infection following an infectious blood meal, ii) disseminate the virus beyond the midgut barrier, and iii) retransmit the virus through the saliva during the next bite. In VCap models, VComp and EIP are often simplified under the EIP₅₀, the time required to reach 50% of infectious mosquitoes. Effectively, each individual mosquito has a given EIP leading to a range of EIPs in the population. EIP distribution can be assessed experimentally by measuring the time between the initial mosquito infection and the mosquito infectiousness using an adequate experimental design (transmission assay for a relevant number of individual mosquitoes and time points). Taking into account the time-dependency of Vcomp improves VCap estimation and therefore allows to capture the full epidemic potential of arboviruses (Lequime et al., 2020). VComp is impacted by biotic (e.g., mosquito and virus genotype, virus dose, mosquito microbiota) and abiotic (e.g., temperature) factors (Viglietta et al., 2021), but how these factors shape VComp dynamics has still to be determined.

Dengue virus (DENV), yellow fever virus (YFV), Zika virus (ZIKV), and chikungunya virus (CHIKV) pose a major sanitary threat as they are responsible for hundreds of millions of human infections each year worldwide, leading to severe morbidity and mortality (Labeaud et al., 2011; Bhatt et al., 2013). These arboviruses are primarily transmitted to humans by *Aedes aegypti* mosquitoes, although the Asian tiger mosquito, *Aedes albopictus*, is often incriminated as a vector. Indeed, *Ae. albopictus* is an important vector of arboviruses as evidenced by vector competence laboratory assays and the detection of infected field specimens (Gratz, 2004; Paupy et al., 2009). Notably, *Ae. albopictus* was identified as the main vector during CHIKV outbreaks in Gabon (2007), Congo (2011) as well as in a major outbreak at La Réunion island (2006) (Schuffenecker et al., 2006; Bonilauri et al., 2008; Pagès et al., 2009; Paupy et al., 2012; Mombouli et al., 2013). In Europe, this vector species is incriminated for autochthonous circulation of CHIKV for instance in Italy (Venturi et al., 2017) and mainland France (Delisle et al., 2015). Vector competence studies established that vector competence of *Ae. albopictus* for CHIKV depends on genetic (e.g., mosquito and virus genotype) and environmental (e.g., temperature) factors (Tsetsarkin et al., 2007; Vazeille et al., 2007; Zouache et al., 2014; Sanchez-Vargas et al., 2019). Host viremia, approximated by virus dose in the blood meal during artificial mosquito infectious feeding experiments, is another major factor that drives mosquito vector competence (Nguyet et al., 2013; Aubry et al., 2020). Vertebrate host viremia for CHIKV last 4 to 12 days with an increase in blood viral titer prior to symptoms appearance, up to a peak around 8 log₁₀ infectious particles/mL followed by a decrease until virus clearance for most of the cases (Schwartz & Albert, 2010). Beyond non-human primates, an estimate of CHIKV human viremia dynamics is lacking due to limited longitudinal monitoring of infected patients, despite it could help to decipher the duration and magnitude of human infectiousness for mosquitoes (Labadie et al., 2010). In *Ae. albopictus*, two studies exposed mosquitoes to a range of CHIKV doses in the blood meal with varying outcomes on vector competence as estimated by mosquito infection and dissemination rate (Pesko et al., 2009; Hurk et al., 2010). Vector competence studies on *Ae. albopictus* from mainland France measured CHIKV transmission rate although upon exposure to a single dose, always above 6.5 log₁₀ FFU/mL range which does not cover the range of human viremia (Moutailler et al., 2009; Vega-Rua et al., 2013; Zouache et al., 2014; Vega-Rúa et al., 2015). In addition, these studies focused on a limited number of time points after CHIKV exposure that prevent to capture the dynamics of vector competence. A study monitoring intra-vector dynamics of CHIKV and its epidemiological relevance is still lacking, notably upon variations of vector competence major drivers such as virus dose.

Here, we studied intra-vector infection dynamics of a field-derived population of *Ae. albopictus* from Lyon metropolis exposed by artificial membrane feeding to a range of human viraemia-like CHIKV (La Réunion 06.21 isolate, East Central South Africa (ECSA) clade) doses, based on our model of human CHIKV viremia in the blood. Strains from ECSA clade carrying the same A226V mutation on envelope *E1* gene than 06.21 were identified from autochthonous cases in mainland France, supporting the choice of the 06.21 strain for this study

99 (Franke et al., 2019). Individual mosquitoes were analyzed from day 2 to day 20 post-exposure (dpe) to
100 determine infection, dissemination, and transmission rates by infectious titration in addition to the
101 quantification of CHIKV RNA load in the saliva. This allowed us to estimate CHIKV intra-vector dynamics and
102 the strength of vector infection, dissemination, and transmission barriers as well as the distribution of EIP
103 according to the virus dose in the blood meal. These data were implemented in the agent-based model *nosoi*
104 (Lequime et al., 2020) to estimate, using realistic vectorial capacity parameters, the epidemic potential of
105 CHIKV in a French population of *Ae. albopictus*. Our results improve our understanding on vector-virus
106 interactions and provides key informations to better anticipate and prevent CHIKV emergence in mainland
107 France.

108 Methods

109 Modelling chikungunya viraemia in humans

110 Chikungunya virus (CHIKV) loads in human blood along with the time course of infection in patients were
111 recovered from two studies. The first study monitored blood CHIKV viraemia from a retrospective cohort of
112 102 febrile patients in Bandung, West Java, Indonesia, between 2005 and 2009 (Riswari et al., 2015). The
113 second study assessed CHIKV RNA viremic profile from 36 sera from day 1 to day 7 of illness during a CHIKV
114 epidemic in Thepa and Chana districts of Songkhla province, Thailand (Appassakij et al., 2013). For the
115 second study, the median value of the blood CHIKV RNA loads from a group of patients (n=2 to 21) per day of
116 illness was used. The viraemia data from RT-qPCR was expressed on the logarithmic scale to the base 10 before
117 model fitting. Wood's gamma-type function was used to model the viraemia dynamic. The function is given in
118 the following equation:

$$119 y(t) = at^b e^{-ct} \text{ (Eq. 1)}$$

120
121 where $y(t)$ represents the level of viraemia in the blood at t days post-infection, with a , b , and c
122 representing constants linked to the viraemia dynamics (Islam et al., 2013). Viraemia data were originally
123 expressed in time pre- or post-symptom onset, while the model represents viraemia as a function of time post-
124 infection. A fixed arbitrary median intrinsic incubation period of 6 days was added to each viraemia time to
125 standardize the time scale between the data and the model. This fixed incubation period falls into the
126 estimated 2-10 days incubation range (Moloney et al., 2014) and was chosen to ensure that all observed
127 viraemia data occurred after infection. The model was fitted to the data using non-linear least-squares
128 regression implemented in the *nls* function in the R environment (RCORETeam, 2022). This method proposed a
129 possible intra-human CHIKV viraemia dynamic with 95% confidence intervals.
130
131

132 CHIKV stock production and titration

133 The CHIKV strain 06.21 from the Indian Ocean lineage was isolated from a newborn serum sample with
134 neonatal encephalopathy in La Réunion island in 2005 (Schuffenecker et al., 2006). This strain was amplified in
135 *Aedes albopictus* cell line C6/36 as previously described (Raquin et al., 2015). CHIKV was inoculated at a
136 multiplicity of infection of 0.01 on *Ae. albopictus* C6/36 cells cultivated in Leibovitz's L-15 media (Gibco) with
137 10 % (v:v) 1X Tryptose Phosphate Broth (Gibco), 10 % (v:v) foetal bovine serum and 0.1 % (v:v) 10,000 units/mL
138 penicillin/streptomycin (Gibco). Cells were incubated for 3 days at 28 °C before the cell supernatant was
139 clarified by centrifugation for 5 min at 500 g and stored at -80 °C as aliquots. CHIKV infectious titer was
140 measured on C6/36 using fluorescent focus assay (Raquin et al., 2015). Briefly, 3×10^5 cells/well were inoculated
141 in 96-well plates (TPP) with 40 μ L/well of viral inoculum (after culture media removal) and incubated for 1 h at
142 28 °C. 150 μ L/well of a mix 1:1 L-15 media and 3.2% medium viscosity carboxymethyl cellulose (Sigma) were
143 added as an overlay before incubation of the cells for 3 days at 28 °C. After incubation, cells were fixed in 150
144 μ L/well of 4 % paraformaldehyde for 20 min at room temperature (RT) and then rinsed 3 times in 100 μ L/well
145 of 1X Dulbecco's phosphate-buffered saline (DPBS) (Gibco) prior to immune labelling. Cells were permeabilized
146 for 30 min in 50 μ L/well of 0.3 % (v:v) Triton X-100 (Sigma) in 1X DPBS + 1 % Bovine Serum Albumin (BSA,
147 Sigma) at RT then rinsed 3 times in 100 μ L/well of 1X DPBS. A Semliki Forest virus anticapsid antibody cross-
148 reacting with CHIKV was used as a primary antibody, diluted 1:600 in 1X DPBS + 1 % BSA (Greiser-Wilke et al.,
149 1989). Cells were incubated in 40 μ L/well of primary antibody for 1 h at 37°C, rinsed 3 times in 100 μ L/well of
150 1X DPBS then incubated in 40 μ L/well of anti-mouse Alexa488 secondary antibody (Life Technologies) at 1:500

151 in 1X DPBS + 1 % BSA for 30 min at 37 °C. Cells were rinsed 3 times in 100 µL/well 1X DPBS, then once in 100
152 µL/well tap water, stored at 4 °C overnight before the enumeration of fluorescent foci under Zeiss Colibri 7
153 fluorescence microscope at 10X objective. The CHIKV infectious titer was expressed as the log₁₀ fluorescent
154 focus unit (FFU) per mL. Plates were then stored at 4 °C protected from light to allow further reading. The
155 infectious titer of the neat CHIKV 06.21 stock was 8.63 log₁₀ FFU/mL.

156

157 **Mosquito colony maintenance**

158 The Lyon metropolis population of *Aedes albopictus* originates from a field sampling of larvae in 2018 that
159 were brought back to insectary for rearing (Microbial Ecology lab, Lyon, France). Sampling locations included
160 Villeurbanne (N : 45°46'18990" E : 4°53'24615") and Pierre-Bénite (N :45°42'11534" E : 4°49'28743") in Lyon
161 metropolis area, mainland France. Mass rearing of the population under standard laboratory conditions (28 °C,
162 80% relative humidity, 16:8 hours light:dark cycles) using mice feeding (*Mus musculus*) allowed to maintain
163 genetic diversity, in accordance with the Institutional Animal Care and Use Committee from Lyon1 University
164 and the French Ministry for Higher Education and Research (Apafis #31807-2021052715018315). Prior to
165 infectious blood feeding, eggs were hatched for 1 h in dechlorinated tap water, and larvae were reared at 26
166 °C (12:12h light:dark cycle) at a density of 200 larvae in 23 x 34 x 7 cm plastic trays (Gilac) in 1.5 L of
167 dechlorinated tap water supplemented with 0.1 g of a 3:1 (TetraMin tropical fish food:Biover yeast) powder
168 every two days. Adults were maintained in 32.5 x 32.5 x 32.5 cm mesh cages (Bugdorm) at 28 °C, 80 % relative
169 humidity, 12:12h light:dark cycle with permanent access to 10% sugar solution.

170

171 **Experimental mosquito exposure to CHIKV**

172 Female mosquitoes (4 to 8-day old) from F₁₀ generation were confined in 136 x 81 mm plastic feeding
173 boxes (Corning-Gosselin) with ~60 individual per box then transferred to the level 3 biosafety facility (SFR
174 Biosciences, AniRA-L3, Lyon Gerland) at 26 °C, 12:12 h light:dark cycle deprived from sugar solution 16 h before
175 the infectious blood meal. The blood meal was composed of a 2:1 (v:v) mixture of washed human erythrocytes
176 (from multiple anonymous donors collected by EFS AURA under the CODECOH agreement DC-2019-3507) and
177 viral suspension at several doses, and supplemented with 2 % (v:v) of 0.5 M ATP, pH 7 in water (Sigma). Feeders
178 (Hemotek) were covered with pig small intestine and filled with 3 mL of infectious blood mixture. Females
179 were allowed to feed for 1 h at 26 °C and blood aliquots were taken before (T0) and after (1h) the feeding and
180 stored at -80 °C for virus titration (Figure S1). Mosquitoes were anaesthetized on ice and fully engorged
181 females were transferred in 1-pint cardboard containers (10-25 females/container) and maintained with 10 %
182 sucrose. Cardboard containers were placed in 18 x 18 x 18 inches cages (BioQuip) and kept in climatic chambers
183 at 26 °C, 70 % humidity. Two independent vector competence experiments were conducted with 370 and 418
184 individuals mosquitoes per experiment, respectively. In a first experiment (n=370), mosquito body and head
185 infection were tested for the presence of infectious virus at 4 time points while in the second experiment
186 (n=418), mosquito head and saliva were analyzed at 10 time points.

187

188 **Mosquito dissection and CHIKV detection**

189 At the selected day post-exposure (dpe) to CHIKV, individual saliva were collected then the heads and
190 bodies were recovered. Prior to saliva collection, mosquitoes were anaesthetized on ice then legs and wings
191 were removed under a stereomicroscope. Individuals were placed on plastic plates maintained by double-
192 sided adhesive tape. The proboscis was inserted in a trimmed 10 µL filtered tip containing 10 µL of foetal
193 bovine serum (FBS) held above the mosquito by modelling clay (Heitmann et al., 2018). Two µL of 1 %
194 pilocarpine hydrochloride (Sigma) supplemented with 0.1 % Tween-20 (Sigma) in water were added on the
195 thorax of each mosquito to enhance salivation. Mosquitoes were allowed to salivate at 26 °C, 80 % relative
196 humidity for 1 h. The FBS that contains the saliva was expelled in an ice-cold tube filled with 150 µL of DMEM
197 media (Gibco) supplemented with antibiotics solution (Amphotericin B 2.5 µg/ml, Nystatin 1/100, Gentamicin
198 50 µg/ml, Penicillin 5 U/ml and Streptomycin 5 µg/ml (Gibco)). Following salivation, each mosquito's head and
199 body were separated using a pin holder with 0.15 mm minutien pins (FST). Heads and bodies were transferred
200 in individual grinding tubes (Qiagen) containing 500 µL of DMEM supplemented with antibiotics (see above)
201 and one 3-mm diameter tungsten bead (Qiagen). Samples were ground on a 96-well adapter set for 2 x 1 min,
202 30 Hz using a TissueLyser II (Qiagen), then stored at -80 °C. CHIKV detection was performed once on 40 µL of
203 undiluted (raw) saliva, head and body samples using fluorescent focus assay on C6/36 cells (see above). Each
204 mosquito sample was declared positive or negative for CHIKV in the presence or absence of a fluorescent

205 signal, respectively. Each 96-well plate contained positive (virus stock) and negative (raw grinding media)
206 controls. Two independent persons examined each plate. Of note, saliva samples were deposited immediately
207 (no freezing step) on C6/36 cells to maximize CHIKV detection. 30 μ L of saliva sample were immediately mixed
208 with 70 μ L of TRIzol (Life Technologies) and stored at -80°C before RNA isolation. The rest of the samples were
209 stored at -80°C as a backup.

210 211 **RNA isolation from saliva**

212 Total RNA was isolated from 30 μ L of saliva mixed with 70 μ L TRIzol and then stored at -80°C , as described
213 (Raquin et al., 2017). After thawing samples on ice, 20 μ L chloroform (Sigma) were added. The tubes were
214 mixed vigorously, incubated at 4°C for 5 min and centrifuged at 17,000 G for 15 min, 4°C . The upper phase
215 was transferred in a new tube containing 60 μ L isopropanol supplemented with 1 μ L GlycoBlue (Life
216 Technologies). Samples were mixed vigorously and stored at -80°C overnight to allow RNA precipitation. After
217 15 min at 17,000 G, 4°C , the supernatant was discarded, and the blue pellet was rinsed with 500 μ L ice-cold
218 70 % ethanol in water. The samples were centrifuged at 17,000 G for 15 min, 4°C , the supernatant was
219 discarded, and the RNA pellet was allowed to dry for 10 min at room temperature. Ten μ L RNase-free water
220 (Gibco) were added, and samples were incubated at 37°C for 10 min to solubilize RNA prior to transfer in
221 RNase-free 96-well plates and storage at -80°C .

222 223 **CHIKV RNA load quantification in saliva**

224 Total RNA (2 μ L) isolated from individual mosquito saliva were used as template in a one-step TaqMan RT-
225 qPCR assay. The QuantiTect Virus kit (Qiagen) was used to prepare the reaction mix in a final volume of 30 μ L.
226 The reaction solution consisted of 6 μ L 5X master mix, 1.5 μ L primers (forward 5'-CCCGGTAAGAGCGGTGAA-3'
227 and reverse 5'-CTTCCGGTATGTCGATGGAGAT-3') and TaqMan probe (5'-6FAM-TGCGCCGTAGGGAACATGCC-
228 BHQ1-3') (Hurk et al., 2010) mixed at 0.4 μ M and 0.2 μ M final concentration respectively, 0.3 μ L 100X RT mix,
229 20.2 μ L RNase-free water (Gibco) and 2 μ L template saliva RNA. RT-qPCR reaction was conducted on a Step
230 One Plus machine (Applied) for 20 min at 50°C (RT step), 5 min at 95°C (initial denaturation) and 40 cycles with
231 15 s at 95°C and 45 s at 60°C . Serial dilutions of CHIKV 06.21 synthetic RNA from 8 to 1 \log_{10} copies/ μ L were
232 used as an external standard to estimate CHIKV RNA copies in saliva samples. Each plate contained duplicates
233 of standard synthetic RNA samples as well as negative controls and random saliva samples without reverse
234 transcriptase (RT-) also in duplicate. Aliquots from the same standard RNA (thawed only once) were used for
235 all the plates, and samples from a single time-point were measured on the same plate to allow sample
236 comparison.

237 238 **Statistical analyses**

239 Mosquito infection (number of CHIKV-positive mosquito bodies / number engorged mosquitoes),
240 dissemination (number of CHIKV-positive heads / number of CHIKV-positive bodies) and transmission rate
241 (number of positive CHIKV-saliva / number of CHIKV-positive heads) were analysed by logistical regression and
242 considered as binary response variables. The time (dpe) and virus dose (\log_{10} FFU/mL) were considered
243 continuous explanatory variables in a full factorial generalized linear model with a binomial error and a logit
244 link function. Logistic regression assumes a saturation level of 100% and could not be used to model the
245 relationship between the probability of transmission (response variable) and the time post-infection, the dose
246 and their interaction (predictors). Therefore, we first estimated the saturation level (K) for each dose and
247 subtracted the value $N = \text{number of mosquitoes with CHIKV dissemination} \times (100\% - K)$ to the number of
248 mosquitoes without virus in their saliva at each time post virus exposure to artificially remove mosquitoes that
249 would never ultimately transmit the virus from the dataset. Logistic regression was then used on these
250 transformed data to predict transmission rates across time post virus exposure and the virus dose (Figure S2).
251 The statistical significance of the predictors' effects was assessed by comparing nested models using deviance
252 analysis based on a chi-squared distribution. All the statistical analyses were performed in R Studio (Posit), and
253 figures were created with the package *ggplot2* within the *Tidyverse* environment (Wickham et al., 2019). The
254 R script used for this study is available, and supplementary table 1 summarizes the proportion of infected,
255 disseminated and infectious mosquitoes for all the experiments conducted.

256 257 **Epidemiological modelling using *nsoi***

258 A series of stochastic agent-based model simulations were performed using the R package *nosoi* and a
259 specific branch available on *nosoi*'s GitHub page (<https://github.com/slequime/nosoi/tree/fontaine>) as
260 previously done (Lequime et al., 2020). Briefly, 100 independent simulations were run in replicates for each
261 condition. Each simulation started with one infected human and was run for 365 days or until the allowed
262 number of infected individuals (100,000 humans or 1,000,000 mosquitoes, respectively) was reached. We
263 considered transmission only between an infected mosquito and an uninfected human or between an infected
264 human and an uninfected mosquito. Vertical and sexual transmission, and the impact of potential
265 superinfection were ignored during the simulations. We assumed no particular structure within host and
266 vector populations.

267 It was also considered that humans do not die from infection and leave the simulation after they clear the
268 infection (here 12 days). Each human agent experienced a Poisson-like distribution of bites per day with a
269 mean value manually set at 1, 2, 3, 4, 5, 6, 7, 8, 9, 10 or 60 based on field measurement of *Aedes albopictus*
270 blood-feeding behaviour (Delatte et al., 2010). Human-to-mosquito transmission followed a time-post-
271 infection-dependent probability function, identical for all human agents, computed from the human viraemic
272 profile (Eq. 1, see above) and dose-response experiments (Eq. 2) :

273

$$274 \quad p_{trans H \rightarrow M}(t) = \frac{1}{1 + \exp(-(-11.1678 + 1.9929 * (a * t^b * \exp(-c * t)))})} \quad (\text{Eq. 2})$$

275 where based on our model, $a = 0.01479$, $b = 7.21809$ and $c = 1.11915$.

276

277 The daily survival probability of infected mosquito agents was set empirically at 0.85 (Favier et al., 2005;
278 Fontaine et al., 2018). Human biting (only one per mosquito agent) was set at fixed dates depending on a
279 gonotrophic cycle duration drawn for each mosquito in a truncated Poisson distribution with a mean of 4 days
280 (no draws below 3). The mosquito-to-human transmission was determined for each mosquito agent based on
281 its individual EIP value acting as a threshold for transmission (if time post-infection is greater or equal to the
282 EIP value, the mosquito can transmit). However, a certain proportion (based on saturation parameter K , see
283 above) of mosquitoes never transmitted. The individual EIP value was dependent on the virus dose that
284 initiated the infection based on this equation (Lequime et al., 2020):

285

$$286 \quad DD50 = \frac{(\log(\frac{-P}{P-1.001}) - \beta_0 - \beta_1 \times X1)}{\beta_2 + \beta_3 \times X1} \quad (\text{Eq. 3})$$

287

288 where $P = 0.5$ (i.e., the median transmission probability), β_0 is the Y-intercept value (-2.328973), β_1
289 (0.278953), β_2 (0.136746) and β_3 (0.003276) are model coefficients associated to the virus dose, time post virus
290 exposure and their interaction, respectively. $X1$ represents the virus dose value.

291

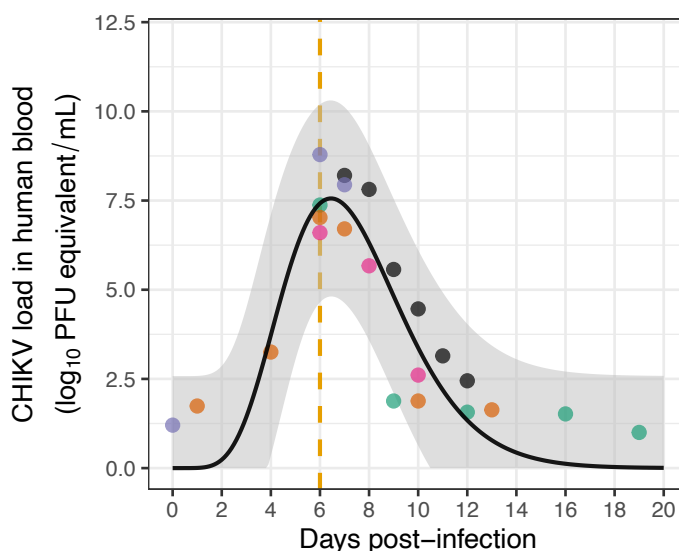
292

Results

293 Estimating CHIKV viraemia in humans by modelisation of clinical data

294 Intra-human dynamic of CHIKV viraemia over time post-infection was approximated using time course of
295 human CHIKV viraemia in individual patients from two studies (Appassakij et al., 2013; Riswari et al., 2015).
296 CHIKV loads were assessed at 3 to 6 different time points, prior or post symptoms onset from the blood of 5
297 patients. The range of CHIKV viraemia duration among the 5 patients was 4-12 days, with a minimal and a
298 maximum CHIKV load of 1 and 8.78 \log_{10} PFU equivalent/mL, respectively. Of note, two patients displayed 1.04
299 and 3.25 \log_{10} PFU equivalent/mL before symptoms onset, respectively. Modelling CHIKV viraemic profile using
300 a Wood's gamma-type function indicates that mean viral load rapidly increases to peak after 6.45 days (i.e.
301 within 24 h after symptoms onset) at 7.55 \log_{10} PFU equivalent/mL (7.01-8.78 \log_{10} equivalent PFU/mL
302 depending on the patient) (Figure 1).

303

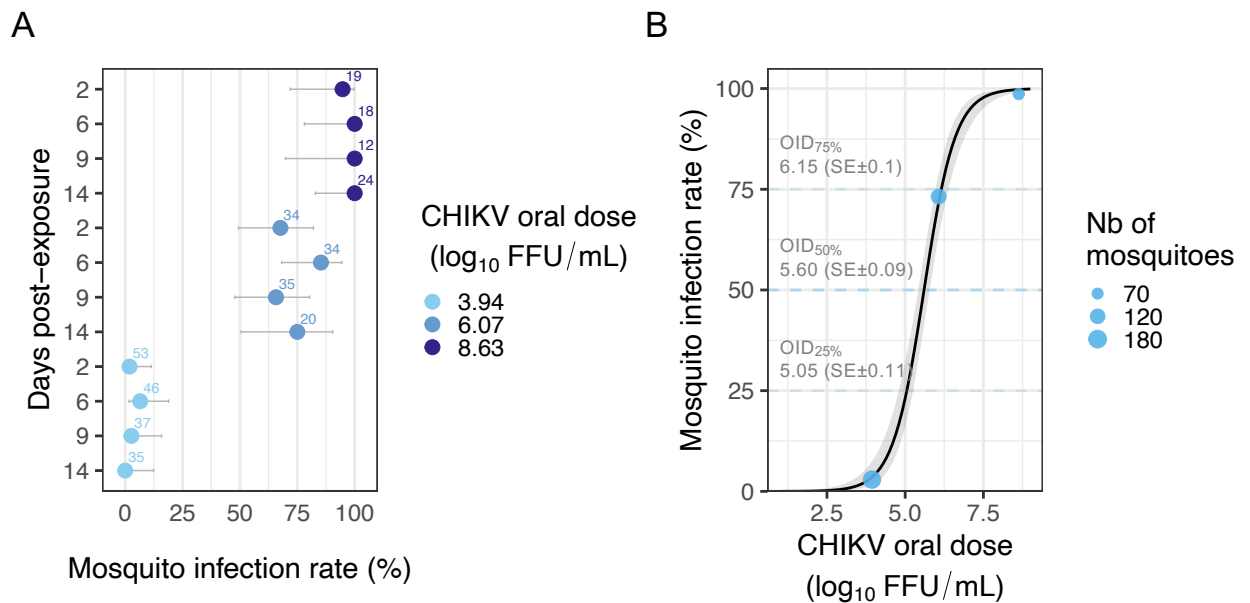


304
305
306
307
308
309
310
311
312
313
314

Figure 1 - Estimated time course of CHIKV load in human blood as a function of days post-infection. A Wood's gamma-type function was used to model CHIKV viraemia dynamics based on the time course of human viraemia data in 5 patients. The black line represents model prediction using mean fit parameter values. Each dot represents a single experimental measurement with colours corresponding to different patients. The vertical gold line indicates the day of symptoms onset. The grey ribbon represents upper and lower predicted values. Refers to raw data table "ChikV_Viremia_dynamic.txt" (see data availability section).

315 **The dose, but not the time, modulates mosquito infection rate**

316 Female *Ae. albopictus* were separately exposed to a human erythrocytes suspension containing three CHIKV
317 doses (3.94, 6.07 and 8.63 log₁₀ FFU/mL) that span the estimated range of human viraemia as estimated above
318 (Figure 1). The mortality rate was very low regardless of time or oral dose, remaining below 5%. Mosquito
319 infection rate (IR) remained below 7 % (n=35 to 53 individuals tested) at 3.94 log₁₀ FFU/mL, ranged from 65 to
320 85 % at 6.07 log₁₀ FFU/mL (n=20 to 35) and raised above 94 % at 8.63 log₁₀ FFU/mL (n=12 to 24) (Figure 2A). A
321 detail table of these data is presented in supplementary table S1. IR significantly increases with the dose but
322 it does not depend on the time post-exposure (Wald χ^2 , $P_{\text{dose}} = 1.1 \times 10^{-6}$, $P_{\text{time}} = 0.9$ and $P_{\text{dose*time}} = 0.17$). As IR
323 depends on the virus dose but not on the time post-exposure, we fitted a logistic model to the data considering
324 CHIKV titer in the blood meal as a unique explanatory variable (Figure 2B). Dose-dependent IR describes a
325 sigmoid with a median oral infection dose (OID_{50%}) of 5.6 log₁₀ FFU/mL and an OID_{25%} and OID_{75%} of 5.05 log₁₀
326 FFU/mL and 6.15 log₁₀ FFU/mL, respectively. The oral infection saturation level was reached at about 7.5 log₁₀
327 FFU/mL.
328



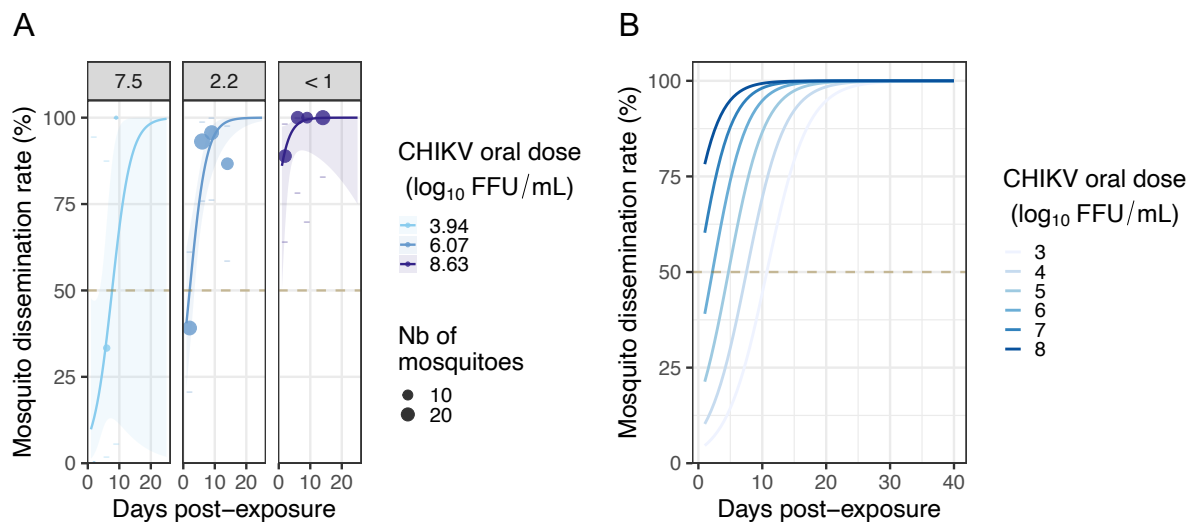
329
330

331 Figure 2 - Dose-dependent infection rate of *Ae. albopictus* mosquitoes exposed to
 332 CHIKV 06.21. (A) The mosquito infection rate corresponds to the proportion (in %) of
 333 mosquito bodies positive for CHIKV infection out of the total of engorged mosquitoes,
 334 measured at 2, 6, 9 and 14 days post-exposure for three CHIKV doses (3.94, 6.07 and 8.63
 335 log₁₀ FFU/mL) in the blood meal. The number of individuals analysed at each time point is
 336 indicated above the bars that represents the 95% confidence interval. (B) Mosquito
 337 infection rate as a function of CHIKV dose in the blood meal. Blue dots correspond to the
 338 observed infection rate upon the three CHIKV doses tested. Dot size is proportional to the
 339 number of mosquitoes tested. The black line was obtained by fitting a logistic model to the
 340 data. The grey ribbon indicates the 95 % confidence interval. The oral infectious dose (OID)
 341 to infect 25 %, 50 % and 75 % of the mosquitoes exposed to CHIKV is indicated with the
 342 associated standard error (in log₁₀ FFU/mL). Refers to raw data table
 343 "Data_titer_EIPdyna_body_head_final.txt" (see data availability section).
 344

345
346

Dose- and time-dependent mosquito dissemination dynamics

347 The proportion of CHIKV-positive heads among positive bodies (*i.e.*, mosquito dissemination rate, DIR) was
 348 analysed using virus dose, time post-exposure and their interaction as explanatory variables. At 2 days post-
 349 exposure, <50 % of the mosquitoes presented a disseminated infection for the doses 3.94 (n=1 individual
 350 tested) and 6.07 (n=18) log₁₀ FFU/mL, whereas DIR was already above 80 % after 2 days in mosquitoes exposed
 351 to 8.63 log₁₀ FFU/mL of CHIKV (n=23) (Figure 3A). Notably, DIR increases >80 % for all the three doses after 6
 352 dpe (n=1 to 29 individual tested per time point and dose) (Figure 3A and Table S1). Although they are not in
 353 interaction, both time and dose impact DIR (Wald χ^2 , $P_{\text{dose}} = 8.29 \times 10^{-6}$, $P_{\text{time}} = 1.75 \times 10^{-6}$ and $P_{\text{dose*time}} = 0.83$).
 354 The plateau was 100 % at doses 3.94 and 8.63 log₁₀ FFU/mL and 95.6% at the dose 6.07 log₁₀ FFU/mL (n=22/23).
 355 The time to reach 50 % dissemination in *Ae. albopictus* exposed to CHIKV was 7.5 days, 2.2 days and <1 day for
 356 3.94, 6.07 and 8.63 log₁₀ FFU/mL CHIKV doses in the blood meal, respectively. DIR was inferred from
 357 experimental data for a larger set of CHIKV dose ranging from 3 to 8 log₁₀ FFU/mL (Figure 3B). All the CHIKV
 358 doses tested led to 100% dissemination within the 40 days range used for predictions, although a longer time
 359 is required to reach this plateau at the lowest dose.



360
361
362
363
364
365
366
367
368
369
370
371
372
373
374
375
376
377
378
379
380
381
382
383
384
385
386
387
388
389
390
391
392
393
394
395
396
397
398
399

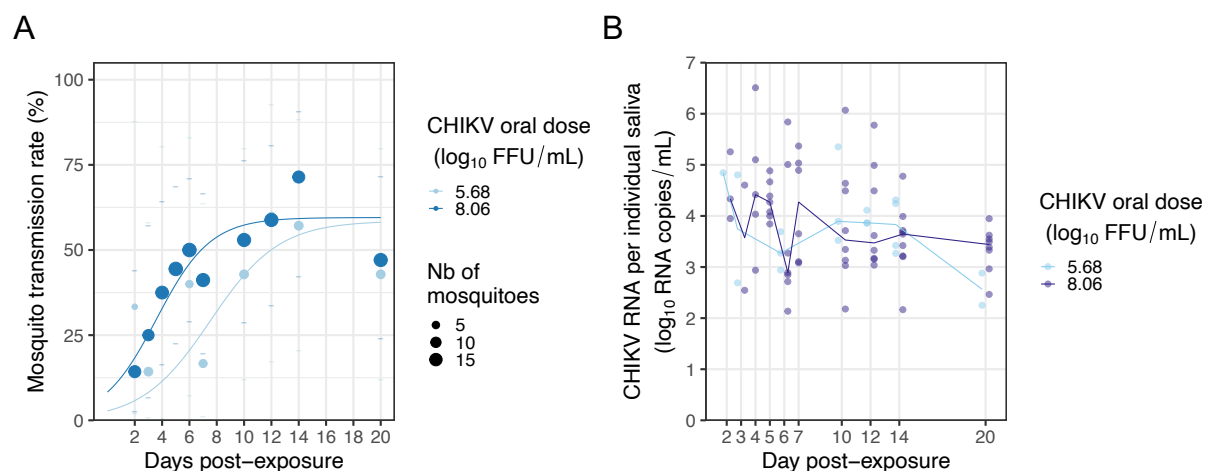
Figure 3 - Dose-dependent dissemination rate of *Ae. albopictus* mosquitoes exposed to CHIKV 06.21. (A) The mosquito dissemination rate corresponds to the number of CHIKV-positive heads out of the infected (CHIKV-positive bodies) individuals, measured at 2, 6, 9 and 14 days post-exposure for three virus doses (3.94, 6.07 and 8.63 log₁₀ FFU/mL) in the blood meal. Dot size is proportional to the number of mosquitoes tested. No disseminated females were detected at day 14 post-exposure at the 3.94 log₁₀ FFU/mL dose. Logistic regression was used to model the time-dependent effect of the virus dose on mosquito dissemination rate. Lines correspond to fit values with their 95% confidence intervals displayed as ribbons. The time needed to reach 50 % dissemination is 7.5, 2.2 and <1 day for the 3.94, 6.07 and 8.63 log₁₀ FFU/mL CHIKV doses, respectively, as indicated within each facet label. (B) Predicted dissemination dynamics according to virus dose and time post-exposure for a range of CHIKV blood meal titers (3 to 8 log₁₀ FFU/mL). Refers to raw data table "Data_titer_EIPdyna_final.txt" (see data availability section).

Time post-exposure modulates transmission rate and viral load in the saliva

The presence of infectious CHIKV particles in individual mosquito saliva collected by forced salivation technique was monitored at a fine time scale. This allowed us to measure the transmission rate (TR) and quantify individual viral load in saliva over time, and to estimate the extrinsic incubation period (EIP). Two virus doses (5.68 and 8.06 log₁₀ FFU/mL) were used to obtain a workable proportion of infectious mosquitoes at a high number of time points that covers mosquito expected lifespan while remaining in the range of human viraemia. From day 2 post-exposure, TR increases following a sigmoid shape, reaching a plateau of around 60% for both doses (Figure 4A). TR was analysed using virus dose, time post-exposure and their interaction as explanatory variables, and only time was significant (Wald χ^2 , $P_{\text{time}} = 0.0037$, $P_{\text{dose}} = 0.18$, and $P_{\text{dose*time}} = 0.8$). Infectious saliva samples were detected as soon as day 2 post-exposure to CHIKV, with a 33 % TR at dose 5.68 log₁₀ FFU/mL (n=1/3 individuals tested) and 14 % at dose 8.06 log₁₀ FFU/mL (n=2/14). The time needed to reach 50 % infectious mosquitoes (*i.e.* Extrinsic Incubation Period 50%, EIP_{50%}) was 7.5 and 3.5 days for doses 5.68 and 8.06 log₁₀ FFU/mL, respectively. A TR saturation at 100 % is a prerequisite to applying logistic regression analysis to the data. Therefore, the proportion of mosquitoes that would not ultimately transmit the virus was artificially removed from the dataset based on the predicted saturation level at each dose (*i.e.*, 40 % of mosquitoes without the virus in their saliva were removed at each time post-infection). Logistic regression was used on these transformed data to predict TR across a range of doses over time (Figure S2).

To decipher if CHIKV load in the saliva could be associated with the virus dose mosquitoes were challenged with, total RNA was isolated at each time point from the saliva of individual mosquitoes exposed to 5.68 or 8.06 log₁₀ FFU/mL. Viral load was measured by TaqMan RT-qPCR assay and analysed according to virus dose and time post-exposure. A high individual variation is noticed (up to 10,000 fold difference between individuals), although CHIKV load in the saliva seems to decrease over time (Figure 4B). Only the time post-exposure significantly affected viral load when considering saliva samples that were CHIKV-positive both in qRT-PCR and in infectious titration (Anova, $P_{\text{time}} = 0.006$, $P_{\text{dose}} = 0.66$ and $P_{\text{dose*time}} = 0.94$). Of note, both time

400 and virus dose affected viral load in the saliva when considering RNA-positive samples regardless of the
401 presence of infectious virus (Figure S3).
402



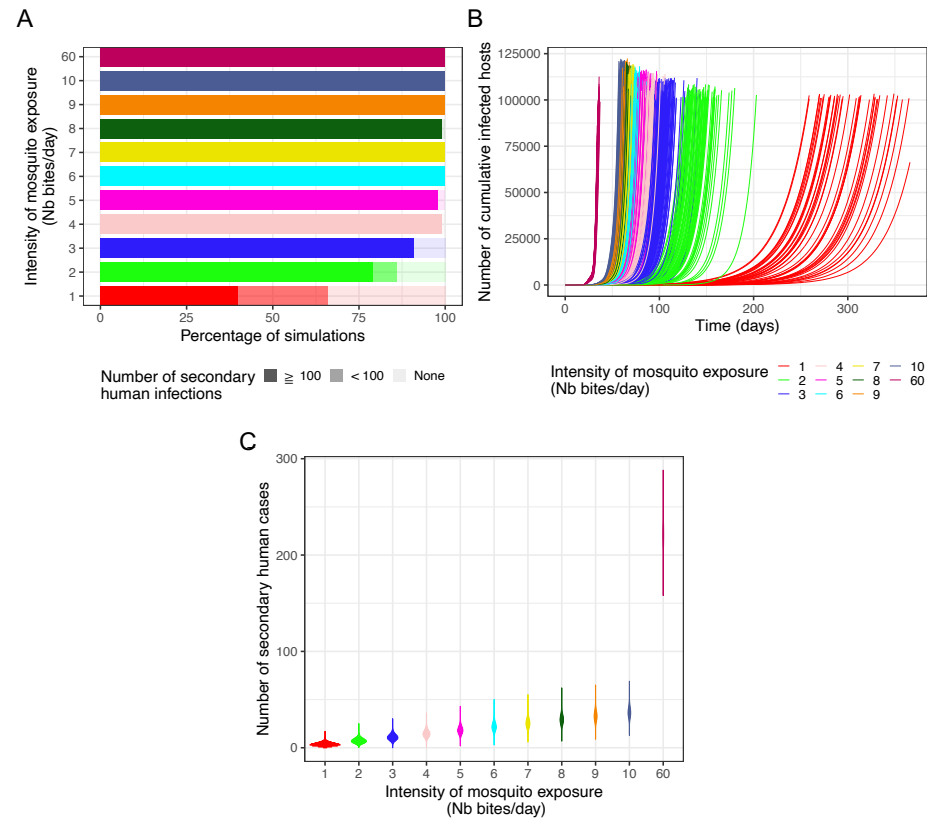
403
404

405 Figure 4 - Transmission dynamics of CHIKV 06.21 by *Ae. albopictus*. (A) Mosquito
406 transmission rate corresponds to the number of CHIKV-positive saliva out of the number
407 of CHIKV-positive heads collected at 2, 3, 4, 5, 6, 7, 10, 12, 14, and 20 days post-exposure
408 for two virus doses (5.68 and 8.06 log₁₀ FFU/mL) in the blood meal. Dot size is proportional
409 to the number of saliva tested. (B) CHIKV RNA load of each saliva scored positive for
410 infectious CHIKV was measured by TaqMan RT-qPCR assay using a synthetic RNA as
411 standard, then expressed in log₁₀ CHIKV RNA copies/saliva. Each dot represents a saliva
412 sample from a mosquito exposed to the indicated dose. Refers to raw data tables
413 “Data_titer_EIPdyna_final.txt” and “Data_CHIKV_RNA_load_saliva.txt” (see data
414 availability section).
415

416

416 Simulation of CHIKV epidemic upon dose-dependent intra-vector dynamics

417 A stochastic agent-based model was used to assess the epidemiological impact of within-host CHIKV
418 dynamics using the R package *nosoi*, as done previously for ZIKV (Lequime et al., 2020). Starting with one
419 infected human in a population of susceptible humans and mosquitoes, the model simulates CHIKV
420 transmissions according to human viraemia, its derived probability of mosquito infection, and virus
421 transmission timeliness (EIP). The model was run 100 independent times for a maximum of 365 days for a
422 range of eleven mean individual mosquito biting rates (1, 2, 3, 4, 5, 6, 7, 8, 9, 10 and 60 independent
423 mosquitoes biting per person per day). Simulations led to large outbreaks (>100 secondary infections) even
424 under a low mosquito biting rate (Figure 5A). The maximum threshold of mosquito infection was reached
425 regardless of biting intensity, although the time needed to reach this threshold and the inter-simulation
426 variation were higher at the lowest biting intensity (*i.e.* 1 bite per day) compare to other conditions (Figure
427 5B). Accordingly, secondary cases values distributions across simulations were narrow for all conditions except
428 at 1 bite per day reflecting the explosive nature of the outbreak. The mean secondary case values increases as
429 a function of the mosquito biting intensity with a mean (\pm SD) of 3.68 (\pm 1.92), 7.37 (\pm 2.71), 11.06 (\pm 3.32),
430 14.75 (\pm 3.84), 18.43 (\pm 4.29), 22.12 (\pm 4.7), 25.81 (\pm 5.07), 29.5 (\pm 5.43), 33.18 (\pm 5.75), 36.87 (\pm 6.07) and
431 221.15 (\pm 6.09) for 1, 2, 3, 4, 5, 6, 7, 8, 9, 10 and 60 mosquito bites per person per day, respectively (Figure 5C).
432



433
434
435
436
437
438
439
440
441
442
443
444
445

Figure 5 - Influence of dose-dependent intra-mosquito CHIKV dynamics on outbreak simulations with various levels of mosquito bites. Stochastic agent-based epidemiological simulations considering within-vector infection dynamics on transmission probability during mosquito-human infectious contacts were performed in 100 independent replicates. A total of 11 mosquito bite intensity levels were tested: 1, 2, 3, 4, 5, 6, 7, 8, 9, 10 and 60 bites per human per day. (A) Stacked proportions of outbreak simulations resulting in no secondary infected human host, < 100 and ≥ 100 infected human hosts. (B) Cumulative number of infected humans over time. Each curve represents a simulation run. (C) Violin plots showing the number of secondary cases densities for each intensity of mosquito exposure. Refers to raw data tables "Compiled_results_run5.csv", "cumulative_run5.csv" and "R0dist_run5.csv" (see data availability section).

447 Vector competence (VComp) of *Aedes albopictus* for chikungunya virus (CHIKV) has been widely
448 studied, notably since the La Réunion outbreak in 2006. Studies outlined a strong impact of mosquito and
449 CHIKV genotype as well as temperature on *Ae. albopictus* potential for CHIKV transmission, including large
450 VComp variations among worldwide *Ae. albopictus* populations exposed to the highly transmissible La
451 Réunion 2006 CHIKV 06.21 isolate (Zouache et al., 2014; Mariconti et al., 2019; Gloria-Soria et al., 2020;
452 Vega-Rúa et al., 2020). However, knowledge gaps remain regarding intra-vector virus dynamics and its
453 impact on CHIKV epidemic potential notably regarding the virus dose. Our work contributes to fill these
454 gaps, providing important data on the interplay between CHIKV and *Ae. albopictus* as well as on the
455 viremia-dependent human infectiousness for mosquitoes.

456

457 Dose and time-dependent barriers to CHIKV intra-vector dynamics

458 *Ae. albopictus* midgut infection is strongly influenced by CHIKV dose in the blood meal. Previous studies
459 documented an oral infectious dose for 50 % of the mosquitoes (OID_{50%}) ranging from 1.7 to 3.52 log₁₀
460 infectious particles per mL of blood for CHIKV 06.21 and thus lower than the 5.60 log₁₀ FFU/mL OID_{50%}
461 estimated in our *Ae. albopictus* population (Tsetsarkin et al., 2007; Pesko et al., 2009; Hurk et al., 2010).
462 ZIKV OID_{50%} was 5.62 log₁₀ FFU/mL in *Ae. albopictus* while in *Ae. aegypti*, ZIKV and DENV OID_{50%} ranged
463 from 4.73 to 8.10 log₁₀ FFU/mL and from 3.95 to 5.5 log₁₀ PFU/mL, respectively (Nguyet et al., 2013; Aubry
464 et al., 2020; Lequime et al., 2020). The CHIKV time-independent infection rate and relatively low OID_{50%} in
465 *Ae. albopictus* suggests that primary infection of midgut cells is rapid and efficient. Such CHIKV midgut
466 infection pattern could be promoted by the presence of several potential midgut receptors for *Alphavirus*
467 entry in mosquitoes (Franz et al., 2015). Importantly, a 0.5 log₁₀ FFU/mL increase in OID_{50%} during the
468 exponential phase results in twice as much infected mosquitoes, which could exacerbate outbreaks,
469 notably upon large vector densities. Therefore, dose-response experiments at a small dose range for each
470 virus and mosquito genotype of interest would significantly improve our understanding of vector
471 competence.

472 According to our results, CHIKV dissemination from the *Ae. albopictus* midgut depends on the
473 interaction between time post-exposure and virus dose. A previous study showed that at day 6 post-
474 exposure, CHIKV dissemination rate in *Ae. albopictus* increases with virus dose, being ~10%, ~50% and
475 >80% upon 3.6, 4.4 and 5.2 log₁₀ PFU/mL in the blood meal respectively (Pesko et al., 2009). Here, we show
476 that if at least 6 days are needed to reach ~30 % dissemination upon 3.94 log₁₀ FFU/mL, virus doses of 6.07
477 and 8.63 log₁₀ FFU/mL led overall to ~90 % dissemination regardless of the time point (except at day 2 for
478 the 6.07 log₁₀ FFU/mL dose where only 40 % dissemination was observed). Of note, CHIKV dissemination
479 rate at 3.94 log₁₀ FFU/mL shall be interpreted with caution due to the low sample size that arise directly
480 from the low infection rate (1.9 to 6.5%, n = 37 to 53 individuals per time point). These results reveal the
481 ability of CHIKV to efficiently disseminate from the midgut, as modelling for a larger dose range estimates
482 that all infected mosquitoes eventually disseminate even at the lowest dose considered (2 log₁₀ FFU/mL).
483 CHIKV and ZIKV present a nearly identical OID_{50%} suggesting similar midgut infection potential in *Ae.*
484 *albopictus*. However, ZIKV dissemination is slower and, to a minor extent, reaches lower value compared
485 to CHIKV (Lequime et al., 2020). This discrepancy might be due to viral replication in the midgut as
486 dissemination rate correlates with midgut viral load (Houk et al., 1981; Bosio et al., 1998; Dickson et al.,
487 2014; Vazeille et al., 2019; Carpenter et al., 2021). CHIKV dissemination might arise from an efficient
488 replication in the midgut tissue. Recently, the CHIKV 3' untranslated region was recently shown to promote
489 dissemination through an increased viral replication in the mosquito midgut (Merwaiss et al., 2020).

490 Ultimately, arboviruses infect and replicate in mosquito salivary glands, this step being essential to
491 allow virus transmission to the host (Vega-Rúa et al., 2015; Raquin & Lambrechts, 2017). Virus prevalence
492 in the head is often used as a proxy for transmission potential but it is likely an overestimate due to salivary
493 glands barriers, notably for CHIKV (Sanchez-Vargas et al., 2021). Our study shows that ~60 % of the
494 mosquitoes with disseminated infection eventually become infectious, this being an underestimate of
495 mosquito-to-host transmission potential due to the use of forced salivation technique (Gloria-Soria et al.,
496 2022). Moreover, transmission rate strongly depends on the time post-exposure. Previously, the time to
497 reach 50 % of infectious mosquitoes in the population (EIP_{50%}) was estimated by a meta-analysis at 7 days
498 (± 1 day), based on dissemination data and for mosquitoes exposed to relatively high virus doses

499 (Christofferson et al., 2014). Despite no overall effect of virus dose on the transmission rate ($P_{\text{dose}} = 0.18$),
500 CHIKV EIP_{50%} was 7.5 and 3.5 days in mosquitoes exposed to 5.68 or 8.06 log₁₀ FFU/mL, respectively,
501 suggesting that virus dose might influence CHIKV transmission. Increasing sample size and/or testing an
502 intermediate virus dose (e.g. 6 log₁₀ FFU/mL) could help to better capture the impact of virus dose on
503 transmission rate and resolve this discrepancy. Interestingly, when considering all CHIKV-positive salivas
504 (including the ones with only CHIKV RNA but found negative during infectious titration), the CHIKV RNA
505 load in the saliva depends on time post-exposure and virus dose but not in interaction. Overall, the CHIKV
506 load in saliva seems higher at high dose but decreases overtime, questioning arbovirus-salivary glands
507 interaction. In a previous study, individual ZIKV-disseminated *Ae. aegypti* mosquitoes were offered
508 successive non-infectious blood meals in an attempt to monitor expelled virus during feeding in a non-
509 sacrificial manner. Authors observed an on/off presence of ZIKV in the blood meal for a single individual
510 over time; however, whether this is due to biological or methodological causes is unclear (Mayton et al.,
511 2021). In *Ae. albopictus*, up to 10,000-fold difference of CHIKV RNA load in the saliva was found between
512 individuals at a given time point and dose, in accordance with previous results (Dubrulle et al., 2009; Bohers
513 et al., 2020; Robison et al., 2020). No correlation was found between CHIKV titer in the salivary glands and
514 in the saliva, that might be linked with such inter-individual variations (Sanchez-Vargas et al., 2019). Despite
515 several studies that identified histological and genetical factors modulating viral infection in this tissue, it
516 is still unclear how and in which amount infectious virions are produced in salivary glands and then
517 transferred into the saliva over time (Ciano et al., 2014; Modahl et al., 2019; Chowdhury et al., 2021;
518 Sanchez-Vargas et al., 2021). Notably, viral particles in the saliva might use specific viral factors and/or
519 mosquito saliva proteins to persist in the saliva and promote their transmission (Pompon et al., 2017;
520 Marin-Lopez et al., 2021). This is key as virus titer in the mosquito inoculum is associated with viraemia
521 level and symptoms severity in mice and macaques models (Labadie et al., 2010; Zhang et al., 2022).
522

523 Genetic and environmental factors impacting intra-vector dynamics

524 VComp is a composite phenotype that also depends on the interaction between virus genotype,
525 mosquito genotype and temperature (Zouache et al., 2014). From a virus perspective, some CHIKV
526 mutations that impact VComp were already described and could be useful for epidemiological monitoring,
527 even if data suggest that overall CHIKV swarm maintains an intermediate mutation frequency to avoid
528 fitness loss in the mosquito (Coffey et al., 2014). Transcriptomics and quantitative genetics studies led to
529 the identification of mosquito genetic loci that constitute interesting targets towards engineered vector
530 control approaches, as shown for *Flaviviridae* (Bosio et al., 2000; Raquin et al., 2017; Aubry et al., 2020;
531 Merklung et al., 2020; Williams et al., 2020; Dong et al., 2022). In addition, mosquitoes host a microbiota
532 composed of bacteria, viruses, fungi and protists that have a major impact on vector's biology (Guégan
533 et al., 2018). Some of these micro-organisms are associated with a decrease in arbovirus transmission and
534 constitute interesting vector control tools, like *Wolbachia* or *Delftia tsuruhatensis* bacteria blocking DENV
535 and *Plasmodium* infection, respectively or insect-specific viruses modulating *Ae. aegypti* vector
536 competence for DENV (Olmo et al., 2018; 2023; Huang et al., 2023). Despite an antiviral activity of
537 *Wolbachia* against CHIKV in *Ae. aegypti*, as well as in *Ae. albopictus* C6/36 cell line, no CHIKV blocking was
538 detected in *Ae. albopictus* mosquitoes (Mousson et al., 2012; Raquin et al., 2015; Aliota et al., 2016).
539 Moreover, *Ae. albopictus* infection by CHIKV impacts mosquito bacterial community composition while
540 several *Ae. albopictus* symbionts were associated with an increase of CHIKV infection (Zouache et al., 2012;
541 Monteiro et al., 2019). The reason for this lack of microbiota-mediated antiviral blocking against CHIKV in
542 *Ae. albopictus* remains obscure, but could depend on mosquito and virus genotype and/or temperature as
543 *Ae. albopictus* microbiota composition depends on the temperature (Bellone et al., 2023). This interaction
544 should be further studied as it could impact arbovirus transmission, as suggested by models estimating
545 that the release of *Wolbachia*-infected *Ae. aegypti* against DENV will be less efficient upon long heatwaves
546 due to loss of *Wolbachia* infection upon high temperatures (Vásquez et al., 2023). With the exception of
547 DENV genotype (Fontaine et al., 2018), the impact of aforementioned factors was not tested on VComp
548 dynamics and it will be interesting to determine if these factors, beyond modulating VComp at discrete
549 time, impact the proportion of infectious mosquitoes over time.
550

551 Human viremia and infectiousness to mosquitoes

552 A large majority of VComp studies exposed *Ae. albopictus* to a high ($>7 \log_{10}$ plaque-forming units
553 (PFU)/mL) CHIKV titer in the blood meal (Coffey et al., 2014). According to our estimate, CHIKV viraemia in
554 humans can reach $>7 \log_{10}$ PFU equivalent per mL of blood, although this corresponds to the highest value
555 measured within a short time window (<2 days). Our CHIKV viraemia estimate from human longitudinal
556 data lasts from 4 to 12 days with a mean maximum titer of $7.55 \log_{10}$ PFU/mL, which is largely supported
557 by previous human and nonhuman studies (Lanciotti et al., 2007; Panning et al., 2008; Labadie et al., 2010;
558 Schwartz & Albert, 2010). The mean human viraemia is above $3.94 \log_{10}$ FFU/mL during 5.5 days, implying
559 that humans are infectious to mosquitoes during more than half of their viraemia. These data are key to
560 improve sanitary guidelines for the management of CHIKV infections and spread. However, major
561 differences in CHIKV viraemia magnitude and length are observed between individual hosts, which can be
562 associated with host and/or virus genotypes as observed in dengue virus (DENV)-infected patients (Nguyet
563 et al., 2013). In addition, if artificial mosquito blood feeding limits variation in blood composition and
564 promotes reproducibility, it does not necessary represent the native infectiousness of human-derived
565 arbovirus for mosquitoes. This is partly linked to host plasma factors level (IgM, IgG, low-density
566 lipoproteins or gamma-aminobutyric acid) while asymptomatic DENV cases are more infectious to
567 mosquitoes than symptomatic counterparts at a given dose suggesting a link between host immune
568 response and vector transmission (Nguyet et al., 2013; Duong et al., 2015; Wagar et al., 2017; Zhu et al.,
569 2017). Moreover, for CHIKV, $\sim 85\%$ infections are symptomatic with a median blood titer about 100-fold
570 higher compare to asymptomatic carriers, although this difference was not statistically significant
571 (Appassakij et al., 2013). Thus, improving epidemiological models by implementing the time-dependant
572 human host infectiousness to mosquitoes represents an interesting lead to better anticipate and prevent
573 CHIKV outbreaks. This notably prompts the need for viraemia monitoring over time in large groups of
574 patients infected by arboviruses, using standardized virus titration procedures to facilitate comparisons
575 and calibrate dose-response experiments in mosquitoes. This also requires other improvements of
576 modelling strategies to account for mosquito and human populations structure, sanitary measures as well
577 as *Ae. albopictus* tendency to take several consecutive blood meals. Indeed, virus dissemination increases
578 with gonotrophic cycles and that successive bloodmeals are associated with a shortened EIP (Delatte et al.,
579 2010; Armstrong et al., 2019; Fikrig & Harrington, 2021; Mulatier et al., 2023). Although those limitations
580 could modulate the explosiveness of the outbreak and could be improved, our data support that CHIKV
581 transmission potential of local *Ae. albopictus* is not a limiting factor for local CHIKV emergence and spread.
582 Finally, such a standardized experimental design can be used to investigate the impact of additional
583 (a)biotic factors on VComp dynamics.

584 Beyond virus dose and time post virus exposure, mosquito and virus genotype, mosquito microbiota
585 and temperature are currently identified as major VComp drivers. Therefore, locally-acquired VComp data
586 from area at risk for arbovirus circulation are needed. This could be achieved by exposing autochthonous
587 field-derived mosquito populations to virus strains currently circulating (or at risk of introduction) upon a
588 range of virus dose and temperature spanning the human viremia and the mosquito season, respectively,
589 while controlling experimentally mosquito microbiota. This is unlikely to be done within a single
590 experiment but will require the incremental acquisition of data sets for each factor, underlying the
591 importance of experimental procedure standardization. Interestingly, modelisation of VComp based on
592 available data could help to target a range of the factor's values to be tested experimentally, as exemplified
593 with temperature (Shocket et al., 2020). These factors act together in interaction making difficult to
594 dissociate their real impact on VComp in the field. Deciphering the complex interplay between each factor
595 on VComp is challenging but feasible (Audsley et al., 2017) and holistic interaction studies could help to
596 address this issue experimentally (Brinker et al., 2019). Beyond experimental conditions, our work
597 underlines that monitoring intra-vector dynamics rather than end-point VComp is key to accurately
598 quantify VComp variations and better estimate VCap (Christofferson & Mores, 2011). Several studies
599 estimated VCap through the lens of mosquito density upon environmental variations (e.g. temperature,
600 micro-climate, land cover) but with limited ecological (mosquito survival rate, biting rate, density per host)
601 and VComp data, notably regarding intra-vector dynamics (Murdock et al., 2017; Wimberly et al., 2020;
602 Peña-García et al., 2023). This highlights the current need for additional VComp and VCap-related studies
603 using field-derived material, as well as increasing efforts between vector biology and modeling fields
604 towards an integrative VCap estimation notably regarding intra-vector arbovirus dynamics. Altogether, this
605 will improve vector control strategies and case management by health authorities.

606

607

Appendices

608 FigS1 - CHIKV infectious titer is stable upon a one hour incubation at 37°C in human erythrocytes
609 suspension. Refers to raw data table “blood_titration_FFU.txt” (see data availability section).

610 FigS2 - Rescaled mosquito transmission dynamics. Refers to raw data table
611 “Data_titer_EIPdyna_final.txt” (see data availability section).

612 FigS3 - Time-course of CHIKV load in mosquito saliva. Refers to raw data table
613 “Data_CHIKV_RNA_load_saliva.txt” (see data availability section).

614 TabS1 - Proportion of infected, disseminated and infectious mosquitoes over time according to the
615 dose of CHIKV in the blood meal. Refers to raw data table “Raw_data_viginier_et_al2023” (see data
616 availability section).

617

618

Acknowledgements

619 This project was funded by the scientific breakthrough project Micro-Be-Have (Microbial impact on
620 insect behavior) of the Université de Lyon within the program Investissements d’Avenir (ANR-11-IDEX-
621 0007; ANR-16-IDEX-0005). We thank the Equipex InfectioTron program and its project manager Isabelle
622 Weiss. We also thank all the members of the Micro-Be-Have consortium for insightful discussions. We
623 thank Anna-Bella Failloux and Patrick Mavingui for the CHIKV 06.21 isolate. We acknowledge the
624 contribution of SFR Biosciences (UAR3444/CNRS, US8/Inserm, ENS de Lyon, UCBL) AniRa biosafety level 3
625 platform (Marie-Pierre Confort) and plateau Analyse Génétique et Cellulaire (Bariza Blanquier) facilities in
626 Lyon. We also thank 2 anonymous reviewers for helpful comments on a previous version of this manuscript.
627

628

Data, scripts, code, and supplementary information availability

629 Data, R scripts, supplementary information and main figures in full size are available online:
630 <https://doi.org/10.5281/zenodo.8033668>

631

632

Conflict of interest disclosure

633 The authors declare that they comply with the PCI rule of having no financial conflicts of interest in
634 relation to the content of the article.

635 Sebastian Lequime is a recommender for PCI infections.

636

Author contributions

637 **BV:** Investigation; Data curation; Validation

638 **LC:** Investigation; Data curation; Validation

639 **CG:** Investigation; Data curation; Validation

640 **EM:** Resources

641 **CM:** Resources

642 **CVM:** Funding acquisition; Resources; Supervision; Writing – review and editing

643 **GM:** Funding acquisition; Writing – review and editing

644 **AF:** Data curation; Formal analysis; Software; Visualization; Methodology; Writing – review and editing

645 **SL:** Data curation; Formal analysis; Software; Visualization; Methodology; Writing – review and editing

646 **MR:** Funding acquisition; Supervision; Writing – review and editing

647 **FA:** Funding acquisition; Project administration; Supervision; Writing – review and editing
648 **VR:** Conceptualization; Investigation; Formal analysis; Data curation; Methodology; Investigation; Project
649 administration; Supervision; Validation; Visualization; Writing – original draft; Writing – review and
650 editing.

651 **Funding**

652 Micro-Be-Have (Microbial impact on insect behavior) of the Université de Lyon within the program
653 Investissements d’Avenir (ANR-11-IDEX-0007; ANR-16-IDEX-0005).

654 **References**

655

656 Aliota MT, Walker EC, Yepes AU, Velez ID, Christensen BM, Osorio JE (2016) The wMel Strain of
657 *Wolbachia* Reduces Transmission of Chikungunya Virus in *Aedes aegypti*. *PLoS neglected tropical*
658 *diseases*, **10**, e0004677. <https://doi.org/10.1371/journal.pntd.0004677>

659 Appassakij H, Khuntikij P, Kemapunmanus M, Wutthananungsan R, Silpapojakul K (2013) Viremic profiles
660 in CHIKV-infected cases. *Transfusion*, **53**, 2567–2574. [https://doi.org/10.1111/j.1537-](https://doi.org/10.1111/j.1537-2995.2012.03960.x)
661 [2995.2012.03960.x](https://doi.org/10.1111/j.1537-2995.2012.03960.x)

662 Armstrong PM, Ehrlich HY, Magalhaes T, Miller MR, Conway PJ, Bransfield A, Misencik MJ, Gloria-Soria A,
663 Warren JL, Andreadis TG, Shepard JJ, Foy BD, Pitzer VE, Brackney DE (2019) Successive blood meals
664 enhance virus dissemination within mosquitoes and increase transmission potential. *Nature*
665 *microbiology*, 1–9. <https://doi.org/10.1038/s41564-019-0619-y>

666 Aubry F, Dabo S, Manet C, Filipović I, Rose NH, Miot EF, Martynow D, Baidaliuk A, Merklings SH, Dickson
667 LB, Crist AB, Anyango VO, Romero-Vivas CM, Vega-Rúa A, Dusfour I, Jiolle D, Paupy C, Mayanja MN,
668 Lutwama JJ, Kohl A, Duong V, Ponlawat A, Sylla M, Akorli J, Otoo S, Lutomiah J, Sang R, Mutebi J-P,
669 Cao-Lormeau V-M, Jarman RG, Diagne CT, Faye O, Sall AA, McBride CS, Montagutelli X, Rašić
670 G, Lambrechts L (2020) Enhanced Zika virus susceptibility of globally invasive *Aedes aegypti*
671 populations. *Science*, **370**, 991–996. <https://doi.org/10.1126/science.abd3663>

672 Audsley MD, Ye YH, McGraw EA (2017) The microbiome composition of *Aedes aegypti* is not critical for
673 *Wolbachia*-mediated inhibition of dengue virus. *PLoS Neglected Tropical Diseases*, **11**, e0005426.
674 <https://doi.org/10.1371/journal.pntd.0005426>

675 Bellone R, Lechat P, Mousson L, Gilbert V, Piorkowski G, Bohers C, Merits A, Kornobis E, Reveillaud J,
676 Paupy C, Vazeille M, Martinet J-P, Madec Y, Lamballerie XD, Duga C, Failloux A-B (2023) Climate
677 change and vector-borne diseases: a multi-omics approach of temperature-induced changes in the
678 mosquito. *Journal of Travel Medicine*, **30**. <https://doi.org/10.1093/jtm/taad062>

679 Bhatt S, Gething PW, Brady OJ, Messina JP, Farlow AW, Moyes CL, Drake JM, Brownstein JS, Hoen AG,
680 Sankoh O, Myers MF, George DB, Jaenisch T, Wint GRW, Simmons CP, Scott TW, Farrar JJ, Hay SI
681 (2013) The global distribution and burden of dengue. *Nature*, **496**, 504–507.
682 <https://doi.org/10.1038/nature12060>

683 Bohers C, Mousson L, Madec Y, Vazeille M, Rhim A, M’ghirbi Y, Bouattour A, Failloux A-B (2020) The
684 recently introduced *Aedes albopictus* in Tunisia has the potential to transmit chikungunya, dengue
685 and Zika viruses. *PLOS Neglected Tropical Diseases*, **14**, e0008475.
686 <https://doi.org/10.1371/journal.pntd.0008475>

- 687 Bonilauri P, Bellini R, Calzolari M, Angelini R, Venturi L, Fallacara F, Cordioli P, Angelini P, Venturelli C,
688 Merialdi G, Dottori M (2008) Chikungunya Virus in *Aedes albopictus*, Italy. *Emerging Infectious*
689 *Diseases*, **14**, 852–854. <https://doi.org/10.3201/eid1405.071144>
- 690 Bosio CF, Beaty BJ, Black WC (1998) Quantitative genetics of vector competence for dengue-2 virus in
691 *Aedes aegypti*. *The American Journal of Tropical Medicine and Hygiene*, **59**, 965–970.
692 <https://doi.org/10.4269/ajtmh.1998.59.965>
- 693 Bosio CF, Fulton RE, Salasek ML, Beaty BJ, Black WC (2000) Quantitative trait loci that control vector
694 competence for dengue-2 virus in the mosquito *Aedes aegypti*. *Genetics*, **156**, 687–698.
695 <https://doi.org/10.1093/genetics/156.2.687>
- 696 Brinker P, Fontaine MC, Beukeboom LW, Salles JF (2019) Host, Symbionts, and the Microbiome: The
697 Missing Tripartite Interaction. *Trends in Microbiology*, **27**, 480–488.
698 <https://doi.org/10.1016/j.tim.2019.02.002>
- 699 Carpenter A, Bryant WB, Santos SR, Clem RJ (2021) Infection of *Aedes aegypti* Mosquitoes with Midgut-
700 Attenuated Sindbis Virus Reduces, but Does Not Eliminate, Disseminated Infection. *Journal of*
701 *Virology*, **95**, e00136-21. <https://doi.org/10.1128/jvi.00136-21>
- 702 Chowdhury A, Modahl CM, Missé D, Kini RM, Pompon J (2021) High resolution proteomics of *Aedes*
703 *aegypti* salivary glands infected with either dengue, Zika or chikungunya viruses identify new virus
704 specific and broad antiviral factors. *Scientific Reports*, **11**, 23696. [https://doi.org/10.1038/s41598-](https://doi.org/10.1038/s41598-021-03211-0)
705 [021-03211-0](https://doi.org/10.1038/s41598-021-03211-0)
- 706 Christofferson RC, Chisenhall DM, Wearing HJ, Mores CN (2014) Chikungunya Viral Fitness Measures
707 within the Vector and Subsequent Transmission Potential. *PLoS ONE*, **9**, e110538.
708 <https://doi.org/10.1371/journal.pone.0110538>
- 709 Christofferson RC, Mores CN (2011) Estimating the Magnitude and Direction of Altered Arbovirus
710 Transmission Due to Viral Phenotype. *PLoS ONE*, **6**, e16298.
711 <https://doi.org/10.1371/journal.pone.0016298>
- 712 Ciano K, Saredy J, Bowers D (2014) Heparan Sulfate Proteoglycan: An Arbovirus Attachment Factor
713 Integral to Mosquito Salivary Gland Ducts. *Viruses*, **6**, 5182–5197. <https://doi.org/10.3390/v6125182>
- 714 Coffey LL, Failloux A-B, Weaver SC (2014) Chikungunya Virus–Vector Interactions. *Viruses*, **6**, 4628–4663.
715 <https://doi.org/10.3390/v6114628>
- 716 Delatte H, Desvars A, Bouétard A, Bord S, Gimonneau G, Vourc’h G, Fontenille D (2010) Blood-Feeding
717 Behavior of *Aedes albopictus*, a Vector of Chikungunya on La Réunion. *Vector-Borne and Zoonotic*
718 *Diseases*, **10**, 249–258. <https://doi.org/10.1089/vbz.2009.0026>
- 719 Delisle E, Rousseau C, Broche B, Leparç-Goffart I, L’Ambert G, Cochet A, Prat C, Foulongne V, Ferré JB,
720 Catelinois O, Flusin O, Tchernonog E, Moussion IE, Wiegandt A, Septfons A, Mendy A, Moyano MB,
721 Laporte L, Maurel J, Jourdain F, Reynes J, Paty MC, Golliot F (2015) Chikungunya outbreak in
722 Montpellier, France, September to October 2014. *Eurosurveillance*, **20**. [https://doi.org/10.2807/1560-](https://doi.org/10.2807/1560-7917.es2015.20.17.21108)
723 [7917.es2015.20.17.21108](https://doi.org/10.2807/1560-7917.es2015.20.17.21108)
- 724 Dickson LB, Sanchez-Vargas I, Sylla M, Fleming K, Black WC (2014) Vector competence in West African
725 *Aedes aegypti* Is Flavivirus species and genotype dependent. *PLoS neglected tropical diseases*, **8**,
726 e3153. <https://doi.org/10.1371/journal.pntd.0003153>

- 727 Dong Y, Dong S, Dizaji NB, Rutkowski N, Pohlenz T, Myles K, Dimopoulos G (2022) The *Aedes aegypti*
728 siRNA pathway mediates broad-spectrum defense against human pathogenic viruses and modulates
729 antibacterial and antifungal defenses. *PLoS Biology*, **20**, e3001668.
730 <https://doi.org/10.1371/journal.pbio.3001668>
- 731 Dubrulle M, Mousson L, Moutailler S, Vazeille M, Failloux A-B (2009) Chikungunya virus and *Aedes*
732 mosquitoes: saliva is infectious as soon as two days after oral infection. *PLoS One*, **4**, e5895.
733 <https://doi.org/10.1371/journal.pone.0005895>
- 734 Duong V, Lambrechts L, Paul RE, Ly S, Lay RS, Long KC, Huy R, Tarantola A, Scott TW, Sakuntabhai A,
735 Buchy P (2015) Asymptomatic humans transmit dengue virus to mosquitoes. *Proceedings of the*
736 *National Academy of Sciences*, **112**, 14688–14693. <https://doi.org/10.1073/pnas.1508114112>
- 737 Favier C, Schmit D, Mller-Graf CDM, Cazelles B, Degallier N, Mondet B, Dubois MA (2005) Influence of
738 spatial heterogeneity on an emerging infectious disease: the case of dengue epidemics. *Proceedings*
739 *of the Royal Society B: Biological Sciences*, **272**, 1171–1177. <https://doi.org/10.1098/rspb.2004.3020>
- 740 Fikrig K, Harrington LC (2021) Understanding and interpreting mosquito blood feeding studies: the case of
741 *Aedes albopictus*. *Trends in Parasitology*, **37**, 959–975. <https://doi.org/10.1016/j.pt.2021.07.013>
- 742 Fontaine A, Lequime S, Moltini-Conclois I, Jiolle D, Leparç-Goffart I, Reiner RC, Lambrechts L (2018)
743 Epidemiological significance of dengue virus genetic variation in mosquito infection dynamics. *PLoS*
744 *Pathogens*, **14**, e1007187. <https://doi.org/10.1371/journal.ppat.1007187>
- 745 Franke F, Giron S, Cochet A, Jeannin C, Leparç-Goffart I, Valk H de, Jourdain F, Lamballerie X de, L'Ambert
746 G, Paty MC (2019) Autochthonous chikungunya and dengue fever outbreak in Mainland France, 2010-
747 2018. *European Journal of Public Health*, **29**. <https://doi.org/10.1093/eurpub/ckz186.628>
- 748 Franz AWE, Kantor AM, Passarelli AL, Clem RJ (2015) Tissue Barriers to Arbovirus Infection in Mosquitoes.
749 *Viruses*, **7**, 3741–3767. <https://doi.org/10.3390/v7072795>
- 750 Gloria-Soria A, Brackney DE, Armstrong PM (2022) Saliva collection via capillary method may
751 underestimate arboviral transmission by mosquitoes. *Parasites & Vectors*, **15**, 103.
752 <https://doi.org/10.1186/s13071-022-05198-7>
- 753 Gloria-Soria A, Payne AF, Bialosuknia SM, Stout J, Mathias N, Eastwood G, Ciota AT, Kramer LD,
754 Armstrong PM (2020) Vector Competence of *Aedes albopictus* Populations from the Northeastern
755 United States for Chikungunya, Dengue, and Zika Viruses. *The American Journal of Tropical Medicine*
756 *and Hygiene*. <https://doi.org/10.4269/ajtmh.20-0874>
- 757 Gratz NG (2004) Critical review of the vector status of *Aedes albopictus*. *Medical and Veterinary*
758 *Entomology*, **18**, 215–227. <https://doi.org/10.1111/j.0269-283x.2004.00513.x>
- 759 Greiser-Wilke I, Moennig V, Kaaden O-R, Figueiredo LTM (1989) Most Alphaviruses Share a Conserved
760 Epitopic Region on Their Nucleocapsid Protein. *Journal of General Virology*, **70**, 743–748.
761 <https://doi.org/10.1099/0022-1317-70-3-743>
- 762 Guégan M, Zouache K, Démichel C, Minard G, Van VT, Potier P, Mavingui P, Moro CV (2018) The mosquito
763 holobiont: fresh insight into mosquito-microbiota interactions. *Microbiome*, **6**, 49.
764 <https://doi.org/10.1186/s40168-018-0435-2>

- 765 Heitmann A, Jansen S, Lühken R, Leggewie M, Schmidt-Chanasit J, Tannich E (2018) Forced Salivation As a
766 Method to Analyze Vector Competence of Mosquitoes. *Journal of Visualized Experiments : JoVE*,
767 57980. <https://doi.org/10.3791/57980>
- 768 Houk EJ, Hardy JL, Presser SB, Kramer LD (1981) Dissemination Barriers for Western Equine
769 Encephalomyelitis Virus in *Culex tarsalis* Infected after Ingestion of Low Viral Doses. *The American*
770 *Journal of Tropical Medicine and Hygiene*, **30**, 190–197. <https://doi.org/10.4269/ajtmh.1981.30.190>
- 771 Huang W, Rodrigues J, Bilgo E, Tormo JR, Challenger JD, Cozar-Gallardo CD, Pérez-Victoria I, Reyes F,
772 Castañeda-Casado P, Gnambani EJ, Hien DF de S, Konkobo M, Urones B, Coppens I, Mendoza-Losana
773 A, Ballell L, Diabate A, Churcher TS, Jacobs-Lorena M (2023) *Delftia tsuruhatensis* TC1 symbiont
774 suppresses malaria transmission by anopheline mosquitoes. *Science*, **381**, 533–540.
775 <https://doi.org/10.1126/science.adf8141>
- 776 Hurk AF van den, Hall-Mendelin S, Pyke AT, Smith GA, Mackenzie JS (2010) Vector Competence of
777 Australian Mosquitoes for Chikungunya Virus. *Vector-Borne and Zoonotic Diseases*, **10**, 489–495.
778 <https://doi.org/10.1089/vbz.2009.0106>
- 779 Islam ZU, Bishop SC, Savill NJ, Rowland RRR, Lunney JK, Tribble B, Doeschl-Wilson AB (2013) Quantitative
780 Analysis of Porcine Reproductive and Respiratory Syndrome (PRRS) Viremia Profiles from
781 Experimental Infection: A Statistical Modelling Approach. *PLoS ONE*, **8**, e83567.
782 <https://doi.org/10.1371/journal.pone.0083567>
- 783 Labadie K, Larcher T, Joubert C, Mannioui A, Delache B, Brochard P, Guigand L, Dubreil L, Lebon P, Verrier
784 B, Lamballerie X de, Suhrbier A, Cherel Y, Grand RL, Roques P (2010) Chikungunya disease in
785 nonhuman primates involves long-term viral persistence in macrophages. *Journal of Clinical*
786 *Investigation*, **120**, 894–906. <https://doi.org/10.1172/jci40104>
- 787 Labeaud AD, Bashir F, King CH (2011) Measuring the burden of arboviral diseases: the spectrum of
788 morbidity and mortality from four prevalent infections. *Population Health Metrics*, **9**, 1.
789 <https://doi.org/10.1186/1478-7954-9-1>
- 790 Lanciotti RS, Kosoy OL, Laven JJ, Panella AJ, Velez JO, Lambert AJ, Campbell GL (2007) Chikungunya virus
791 in US travelers returning from India, 2006. *Emerging Infectious Diseases*, **13**, 764–767.
792 <https://doi.org/10.3201/eid1305.070015>
- 793 Lequime S, Bastide P, Dellicour S, Lemey P, Baele G (2020) nosoi: A stochastic agent-based transmission
794 chain simulation framework in r. *Methods in Ecology and Evolution*, **11**, 1002–1007.
795 <https://doi.org/10.1111/2041-210x.13422>
- 796 Lequime S, Dehecq J-S, Matheus S, Laval F de, Almeras L, Briolant S, Fontaine A (2020) Modeling intra-
797 mosquito dynamics of Zika virus and its dose-dependence confirms the low epidemic potential of
798 *Aedes albopictus*. *PLOS Pathogens*, **16**, e1009068. <https://doi.org/10.1371/journal.ppat.1009068>
- 799 Mariconti M, Obadia T, Mousson L, Malacrida A, Gasperi G, Failloux A-B, Yen P-S (2019) Estimating the
800 risk of arbovirus transmission in Southern Europe using vector competence data. *Scientific Reports*, **9**,
801 17852. <https://doi.org/10.1038/s41598-019-54395-5>
- 802 Marin-Lopez A, Jiang J, Wang Y, Cao Y, MacNeil T, Hastings AK, Fikrig E (2021) *Aedes aegypti* SNAP and a
803 calcium transporter ATPase influence dengue virus dissemination. *PLoS Neglected Tropical Diseases*,
804 **15**, e0009442. <https://doi.org/10.1371/journal.pntd.0009442>

- 805 Mayton EH, Hernandez HM, Vitek CJ, Christofferson RC (2021) A Method for Repeated, Longitudinal
806 Sampling of Individual *Aedes aegypti* for Transmission Potential of Arboviruses. *Insects*, **12**, 292.
807 <https://doi.org/10.3390/insects12040292>
- 808 Merklings SH, Raquin V, Dabo S, Henrion-Lacritick A, Blanc H, Moltini-Conclois I, Frangeul L, Varet H, Saleh
809 M-C, Lambrechts L (2020) Tudor-SN Promotes Early Replication of Dengue Virus in the *Aedes aegypti*
810 Midgut. *iScience*, **23**, 100870. <https://doi.org/10.1016/j.isci.2020.100870>
- 811 Merwaiss F, Filomatori CV, Susuki Y, Bardossy ES, Alvarez DE, Saleh M-C (2020) Chikungunya virus
812 replication rate determines the capacity of crossing tissue barriers in mosquitoes. *Journal of Virology*,
813 **95**. <https://doi.org/10.1128/jvi.01956-20>
- 814 Modahl C, Chowdhury A, Oliveira F, Kini RM, Pompon J (2019) Salivary gland RNA-seq from arbovirus-
815 infected *Aedes aegypti* and *Aedes albopictus* provides insights into virus transmission. *Access*
816 *Microbiology*, **1**. <https://doi.org/10.1099/acmi.imav2019.po0039>
- 817 Moloney RM, Kmush B, Rudolph KE, Cummings DAT, Lessler J (2014) Incubation Periods of Mosquito-
818 Borne Viral Infections: A Systematic Review. *The American Journal of Tropical Medicine and Hygiene*,
819 **90**, 882–891. <https://doi.org/10.4269/ajtmh.13-0403>
- 820 Mombouli J-V, Bitsindou P, Elion DOA, Grolla A, Feldmann H, Niama FR, Parra H-J, Munster VJ (2013)
821 Chikungunya Virus Infection, Brazzaville, Republic of Congo, 2011. *Emerging Infectious Diseases*, **19**,
822 1542–1543. <https://doi.org/10.3201/eid1909.130451>
- 823 Monteiro VVS, Navegantes-Lima KC, Lemos AB de, Silva GL da, Gomes R de S, Reis JF, Junior LCR, Silva OS
824 da, Romão PRT, Monteiro MC (2019) *Aedes*–Chikungunya Virus Interaction: Key Role of Vector
825 Midguts Microbiota and Its Saliva in the Host Infection. *Frontiers in Microbiology*, **10**, 492.
826 <https://doi.org/10.3389/fmicb.2019.00492>
- 827 Mousson L, Zouache K, Arias-Goeta C, Raquin V, Mavingui P, Failloux A-B (2012) The native *Wolbachia*
828 symbionts limit transmission of dengue virus in *Aedes albopictus*. *PLoS neglected tropical diseases*, **6**,
829 e1989. <https://doi.org/10.1371/journal.pntd.0001989>
- 830 Moutailler S, Barré H, Vazeille M, Failloux A (2009) Recently introduced *Aedes albopictus* in Corsica is
831 competent to Chikungunya virus and in a lesser extent to dengue virus. *Tropical Medicine &*
832 *International Health*, **14**, 1105–1109. <https://doi.org/10.1111/j.1365-3156.2009.02320.x>
- 833 Mulatier M, Boullis A, Dollin C, Cebrián-Torrejón G, Vega-Rúa A (2023) Chikungunya Virus Infection and
834 Gonotrophic Cycle Shape *Aedes aegypti* Oviposition Behavior and Preferences. *Viruses*, **15**, 1043.
835 <https://doi.org/10.3390/v15051043>
- 836 Murdock CC, Evans MV, McClanahan TD, Miazgowicz KL, Tesla B (2017) Fine-scale variation in
837 microclimate across an urban landscape shapes variation in mosquito population dynamics and the
838 potential of *Aedes albopictus* to transmit arboviral disease. *PLoS Neglected Tropical Diseases*, **11**,
839 e0005640. <https://doi.org/10.1371/journal.pntd.0005640>
- 840 Nguyet MN, Duong THK, Trung VT, Nguyen THQ, Tran CNB, Long VT, Dui LT, Nguyen HL, Farrar JJ, Holmes
841 EC, Rabaa MA, Bryant JE, Nguyen TT, Nguyen HTC, Nguyen LTH, Pham MP, Nguyen HT, Luong TTH,
842 Wills B, Nguyen CVV, Wolbers M, Simmons CP (2013) Host and viral features of human dengue cases
843 shape the population of infected and infectious *Aedes aegypti* mosquitoes. *Proceedings of the*
844 *National Academy of Sciences of the United States of America*, **110**, 9072–9077.
845 <https://doi.org/10.1073/pnas.1303395110>

- 846 Olmo RP, Ferreira AGA, Izidoro-Toledo TC, Aguiar ERGR, Faria IJS de, Souza KPR de, Osório KP, Kuhn L,
847 Hammann P, Andrade EG de, Todjro YM, Rocha MN, Leite THJF, Amadou SCG, Armache JN, Paro S,
848 Oliveira CD de, Carvalho FD, Moreira LA, Marois E, Imler J-L, Marques JT (2018) Control of dengue
849 virus in the midgut of *Aedes aegypti* by ectopic expression of the dsRNA-binding protein Loqs2.
850 *Nature Microbiology*, **3**, 1385–1393. <https://doi.org/10.1038/s41564-018-0268-6>
- 851 Olmo RP, Todjro YMH, Aguiar ERGR, Almeida JPP de, Ferreira FV, Armache JN, Faria IJS de, Ferreira AGA,
852 Amadou SCG, Silva ATS, Souza KPR de, Vilela APP, Babarit A, Tan CH, Diallo M, Gaye A, Paupy C,
853 Obame-Nkoghe J, Visser TM, Koenraad CJM, Wongsokarijo MA, Cruz ALC, Prieto MT, Parra MCP,
854 Nogueira ML, Avelino-Silva V, Mota RN, Borges MAZ, Drumond BP, Kroon EG, Recker M, Sedda L,
855 Marois E, Imler J-L, Marques JT (2023) Mosquito vector competence for dengue is modulated by
856 insect-specific viruses. *Nature Microbiology*, **8**, 135–149. <https://doi.org/10.1038/s41564-022-01289-4>
857
- 858 Pagès F, Peyrefitte CN, Mve MT, Jarjaval F, Brisse S, Iteaman I, Gravier P, Tolou H, Nkoghe D, Grandadam
859 M (2009) *Aedes albopictus* Mosquito: The Main Vector of the 2007 Chikungunya Outbreak in Gabon.
860 *PLoS ONE*, **4**, e4691. <https://doi.org/10.1371/journal.pone.0004691>
- 861 Panning M, Grywna K, Esbroeck M van, Emmerich P, Drosten C (2008) Chikungunya fever in travelers
862 returning to Europe from the Indian Ocean region, 2006. *Emerging Infectious Diseases*, **14**, 416–422.
863 <https://doi.org/10.3201/eid1403.070906>
- 864 Paupy C, Delatte H, Bagny L, Corbel V, Fontenille D (2009) *Aedes albopictus*, an arbovirus vector: from the
865 darkness to the light. *Microbes and Infection / Institut Pasteur*, **11**, 1177–1185.
866 <https://doi.org/10.1016/j.micinf.2009.05.005>
- 867 Paupy C, Kassa FK, Caron M, Nkoghé D, Leroy EM (2012) A Chikungunya Outbreak Associated with the
868 Vector *Aedes albopictus* in Remote Villages of Gabon. *Vector-Borne and Zoonotic Diseases*, **12**, 167–
869 169. <https://doi.org/10.1089/vbz.2011.0736>
- 870 Peña-García VH, Luvall JC, Christofferson RC (2023) Arbovirus Transmission Predictions Are Affected by
871 Both Temperature Data Source and Modeling Methodologies across Cities in Colombia.
872 *Microorganisms*, **11**, 1249. <https://doi.org/10.3390/microorganisms11051249>
- 873 Pesko K, Westbrook CJ, Mores CN, Lounibos LP, Reiskind MH (2009) Effects of Infectious Virus Dose and
874 Bloodmeal Delivery Method on Susceptibility of *Aedes aegypti* and *Aedes albopictus* to Chikungunya
875 Virus. *Journal of Medical Entomology*, **46**, 395–399. <https://doi.org/10.1603/033.046.0228>
- 876 Pompon J, Manuel M, Ng GK, Wong B, Shan C, Manokaran G, Soto-Acosta R, Bradrick SS, Ooi EE, Missé D,
877 Shi P-Y, Garcia-Blanco MA (2017) Dengue subgenomic flaviviral RNA disrupts immunity in mosquito
878 salivary glands to increase virus transmission. *PLoS Pathogens*, **13**, e1006535.
879 <https://doi.org/10.1371/journal.ppat.1006535>
- 880 Raquin V, Lambrechts L (2017) Dengue virus replicates and accumulates in *Aedes aegypti* salivary glands.
881 *Virology*, **507**, 75–81. <https://doi.org/10.1016/j.virol.2017.04.009>
- 882 Raquin V, Merklung SH, Gausson V, Moltini-Conclois I, Frangeul L, Varet H, Dillies M-A, Saleh M-C,
883 Lambrechts L (2017) Individual co-variation between viral RNA load and gene expression reveals novel
884 host factors during early dengue virus infection of the *Aedes aegypti* midgut. *PLoS Neglected Tropical
885 Diseases*, **11**, e0006152. <https://doi.org/10.1371/journal.pntd.0006152>

- 886 Raquin V, Moro CV, Saucereau Y, Tran F-H, Potier P, Mavingui P (2015) Native *Wolbachia* from *Aedes*
887 *albopictus* Blocks Chikungunya Virus Infection *In Cellulo*. *PLOS ONE*, **10**, e0125066.
888 <https://doi.org/10.1371/journal.pone.0125066>
- 889 RCoreTeam (2022) R Core Team (2021) R: A Language and Environment for Statistical Computing.
- 890 Riswari SF, Ma'roef CN, Djauhari H, Kosasih H, Perkasa A, Yudhaputri FA, Artika IM, Williams M, Ven A van
891 der, Myint KS, Alisjahbana B, Ledermann JP, Powers AM, Jaya UA (2015) Study of viremic profile in
892 febrile specimens of chikungunya in Bandung, Indonesia. *Journal of clinical virology : the official*
893 *publication of the Pan American Society for Clinical Virology*, **74**, 61–5.
894 <https://doi.org/10.1016/j.jcv.2015.11.017>
- 895 Robison A, Young MC, Byas AD, Rückert C, Ebel GD (2020) Comparison of Chikungunya Virus and Zika
896 Virus Replication and Transmission Dynamics in *Aedes aegypti* Mosquitoes. *The American journal of*
897 *tropical medicine and hygiene*. <https://doi.org/10.4269/ajtmh.20-0143>
- 898 Sanchez-Vargas I, Harrington LC, Black WC, Olson KE (2019) Analysis of Salivary Glands and Saliva from
899 *Aedes albopictus* and *Aedes aegypti* Infected with Chikungunya Viruses. *Insects*, **10**, 39.
900 <https://doi.org/10.3390/insects10020039>
- 901 Sanchez-Vargas I, Olson KE, Black WC (2021) The Genetic Basis for Salivary Gland Barriers to Arboviral
902 Transmission. *Insects*, **12**, 73. <https://doi.org/10.3390/insects12010073>
- 903 Schuffenecker I, Iteman I, Michault A, Murri S, Frangeul L, Vaney M-C, Lavenir R, Pardigon N, Reynes J-M,
904 Pettinelli F, Biscornet L, Diancourt L, Michel S, Duquerroy S, Guigon G, Frenkiel M-P, Bréhin A-C,
905 Cubito N, Desprès P, Kunst F, Rey FA, Zeller H, Brisse S (2006) Genome Microevolution of Chikungunya
906 Viruses Causing the Indian Ocean Outbreak. *PLoS Medicine*, **3**, e263.
907 <https://doi.org/10.1371/journal.pmed.0030263>
- 908 Schwartz O, Albert ML (2010) Biology and pathogenesis of chikungunya virus. *Nature Reviews*
909 *Microbiology*, **8**, 491–500. <https://doi.org/10.1038/nrmicro2368>
- 910 Shocket MS, Verwillow AB, Numazu MG, Slamani H, Cohen JM, Moustaid FE, Rohr J, Johnson LR,
911 Mordecai EA (2020) Transmission of West Nile and five other temperate mosquito-borne viruses
912 peaks at temperatures between 23°C and 26°C. *eLife*, **9**, e58511. <https://doi.org/10.7554/elife.58511>
- 913 Smith DL, Battle KE, Hay SI, Barker CM, Scott TW, McKenzie FE (2012) Ross, Macdonald, and a Theory for
914 the Dynamics and Control of Mosquito-Transmitted Pathogens. *PLoS Pathogens*, **8**, e1002588.
915 <https://doi.org/10.1371/journal.ppat.1002588>
- 916 Tsetsarkin KA, Vanlandingham DL, McGee CE, Higgs S (2007) A single mutation in chikungunya virus
917 affects vector specificity and epidemic potential. *PLoS pathogens*, **3**, e201.
918 <https://doi.org/10.1371/journal.ppat.0030201>
- 919 Vásquez VN, Kueppers LM, Rašić G, Marshall JM (2023) wMel replacement of dengue-competent
920 mosquitoes is robust to near-term climate change. *Nature Climate Change*, **13**, 848–855.
921 <https://doi.org/10.1038/s41558-023-01746-w>
- 922 Vazeille M, Madec Y, Mousson L, Bellone R, Barré-Cardi H, Sousa CA, Jiolle D, Yébakima A, Lamballerie X
923 de, Failloux A-B (2019) Zika virus threshold determines transmission by European *Aedes albopictus*
924 mosquitoes. *Emerging Microbes & Infections*, **8**, 1668–1678.
925 <https://doi.org/10.1080/22221751.2019.1689797>

- 926 Vazeille M, Moutailler S, Coudrier D, Rousseaux C, Khun H, Huerre M, Thiria J, Dehecq J-S, Fontenille D,
927 Schuffenecker I, Despres P, Failloux A-B (2007) Two Chikungunya Isolates from the Outbreak of La
928 Reunion (Indian Ocean) Exhibit Different Patterns of Infection in the Mosquito, *Aedes albopictus*. *PLoS*
929 *ONE*, **2**, e1168. <https://doi.org/10.1371/journal.pone.0001168>
- 930 Vega-Rúa A, Lourenço-de-Oliveira R, Mousson L, Vazeille M, Fuchs S, Yébakima A, Gustave J, Girod R,
931 Dusfour I, Leparç-Goffart I, Vanlandingham DL, Huang Y-JS, Lounibos LP, Ali SM, Nougairède A,
932 Lamballerie X de, Failloux A-B (2015) Chikungunya Virus Transmission Potential by Local *Aedes*
933 Mosquitoes in the Americas and Europe. *PLoS Neglected Tropical Diseases*, **9**, e0003780.
934 <https://doi.org/10.1371/journal.pntd.0003780>
- 935 Vega-Rúa A, Marconcini M, Madec Y, Manni M, Carraretto D, Gomulski LM, Gasperi G, Failloux A-B,
936 Malacrida AR (2020) Vector competence of *Aedes albopictus* populations for chikungunya virus is
937 shaped by their demographic history. *Communications Biology*, **3**, 326.
938 <https://doi.org/10.1038/s42003-020-1046-6>
- 939 Vega-Rúa A, Schmitt C, Bonne I, Locker JK, Failloux A-B (2015) Chikungunya Virus Replication in Salivary
940 Glands of the Mosquito *Aedes albopictus*. *Viruses*, **7**, 5902–5907. <https://doi.org/10.3390/v7112917>
- 941 Vega-Rúa A, Zouache K, Caro V, Diancourt L, Delaunay P, Grandadam M, Failloux A-B (2013) High
942 Efficiency of Temperate *Aedes albopictus* to Transmit Chikungunya and Dengue Viruses in the
943 Southeast of France. *PLoS ONE*, **8**, e59716. <https://doi.org/10.1371/journal.pone.0059716>
- 944 Venturi G, Luca MD, Fortuna C, Remoli ME, Riccardo F, Severini F, Toma L, Manso MD, Benedetti E,
945 Caporali MG, Amendola A, Fiorentini C, Liberato CD, Giammattei R, Romi R, Pezzotti P, Rezza G, Rizzo
946 C (2017) Detection of a chikungunya outbreak in Central Italy, August to September 2017.
947 *Eurosurveillance*, **22**, 17–00646. <https://doi.org/10.2807/1560-7917.es.2017.22.39.17-00646>
- 948 Viglietta M, Bellone R, Blisnick AA, Failloux A-B (2021) Vector Specificity of Arbovirus Transmission.
949 *Frontiers in Microbiology*, **12**, 773211. <https://doi.org/10.3389/fmicb.2021.773211>
- 950 Wagar ZL, Tree MO, Mpoy MC, Conway MJ (2017) Low density lipopolyprotein inhibits *flavivirus*
951 acquisition in *Aedes aegypti*. *Insect Molecular Biology*, **26**, 734–742.
952 <https://doi.org/10.1111/imb.12334>
- 953 Wickham H, Averick M, Bryan J, Chang W, McGowan L, François R, Golemund G, Hayes A, Henry L,
954 Hester J, Kuhn M, Pedersen T, Miller E, Bache S, Müller K, Ooms J, Robinson D, Seidel D, Spinu V,
955 Takahashi K, Vaughan D, Wilke C, Woo K, Yutani H (2019) Welcome to the Tidyverse. *Journal of Open*
956 *Source Software*, **4**, 1686. <https://doi.org/10.21105/joss.01686>
- 957 Williams AE, Franz AWE, Reid WR, Olson KE (2020) Antiviral Effectors and Gene Drive Strategies for
958 Mosquito Population Suppression or Replacement to Mitigate Arbovirus Transmission by *Aedes*
959 *aegypti*. *Insects*, **11**, 52. <https://doi.org/10.3390/insects11010052>
- 960 Wimberly MC, Davis JK, Evans MV, Hess A, Newberry PM, Solano-Asamoah N, Murdock CC (2020) Land
961 cover affects microclimate and temperature suitability for arbovirus transmission in an urban
962 landscape. *PLoS Neglected Tropical Diseases*, **14**, e0008614.
963 <https://doi.org/10.1371/journal.pntd.0008614>
- 964 Zhang Y, Yan H, Li X, Zhou D, Zhong M, Yang J, Zhao B, Fan X, Fan J, Shu J, Lu M, Jin X, Zhang E, Yan H
965 (2022) A high-dose inoculum size results in persistent viral infection and arthritis in mice infected with
966 chikungunya virus. *PLoS Neglected Tropical Diseases*, **16**, e0010149.
967 <https://doi.org/10.1371/journal.pntd.0010149>

- 968 Zhu Y, Zhang R, Zhang B, Zhao T, Wang P, Liang G, Cheng G (2017) Blood meal acquisition enhances
969 arbovirus replication in mosquitoes through activation of the GABAergic system. *Nature*
970 *Communications*, **8**, 1262. <https://doi.org/10.1038/s41467-017-01244-6>
- 971 Zouache K, Fontaine A, Vega-Rua A, Mousson L, Thiberge J-M, Lourenco-De-Oliveira R, Caro V,
972 Lambrechts L, Failloux A-B (2014) Three-way interactions between mosquito population, viral strain
973 and temperature underlying chikungunya virus transmission potential. *Proceedings of the Royal*
974 *Society B: Biological Sciences*, **281**, 20141078. <https://doi.org/10.1098/rspb.2014.1078>
- 975 Zouache K, Michelland RJ, Failloux A-B, Grundmann GL, Mavingui P (2012) Chikungunya virus impacts the
976 diversity of symbiotic bacteria in mosquito vector. *Molecular Ecology*, **21**, 2297–2309.
977 <https://doi.org/10.1111/j.1365-294x.2012.05526.x>
- 978